Interaction Notes

Note 535

13 January, 1998

Various Ways to Think of the Resolution of the BLT Equation with an LU Technique

Jean-Philippe Parmantier(*), Xavier Ferrières, Solange Bertuol
ONERA, 8 rue des Vertugadins, 92190 Meudon, FRANCE

and Carl E. Baum
Air Force Research Laboratory/DEHP, bldg. 909, 3550 Aberdeen Ave., KAFB NM 87117, USA

Abstract

The paper presents different properties of the BLT equation and its generalization to the compacting of subnetworks.

With the same routine used to solve a BLT equation, scattering parameters and equivalent sources can be derived for any subnetwork. The well-known LU numerical method is used to solve the BLT equation. Flow graph theory is used to analyze the solution. Similarities to Mason's rules, used in electric circuit theory and automatism, are mentioned pointing out the specificity of the BLT equation. The paper also demonstrates that the LU process is equivalent to a junction-to-junction subnetwork compacting.

The sparse structure of this equation allows several computation improvements, providing significant reduction of memory requirement and calculation time. Due to its particular formulation, several block calculations can be avoided. Moreover, the junction-to-junction compacting process hidden in the LU process suggests an intuitive way to label the waves on a network and to reduce the number of fill-in terms created.

Key words :
Electromagnetic Topology ; Linear Systems ; LU Technique ; Sparse Matrices ; Networks ; Scattering Parameters ; Transmission Lines ; Electromagnetic Compatibility ; Electromagnetic Coupling

* Currently on exchange assignment at Air Force Research Laboratory/DEHP, bldg. 909, 3550 Aberdeen Ave., KAFB NM 87117, USA. This work has been made possible thanks to the Prospective Terms of DGA and AFOSR.

Interaction Notes

Note 535

13 January, 1998

Various Ways to Think of the Resolution of the BLT Equation with an LU Technique

Jean-Philippe Parmantier[*], Xavier Ferrières, Solange Bertuol
ONERA, 8 rue des Vertugadins, 92190 Meudon, FRANCE

and Carl E. Baum
Air Force Research Laboratory/DEHP, bldg. 909, 3550 Aberdeen Ave., KAFB NM 87117, USA

Abstract

This paper presents different properties of the BLT equation and its generalization to the compacting of subnetworks.

With the same routine used to solve a BLT equation, scattering parameters and equivalent sources can be derived for any subnetwork. The well-known LU numerical method is used to solve the BLT equation. Flow-graph theory it used to analyze the solution. Similarities to Mason's rules, used in electric circuit theory and automatism, are mentioned pointing out the specificity of the BLT equation. The paper also demonstrates that the LU process is equivalent to a junction-to-junction subnetwork compacting.

The sparse structure of this equation allows several computation improvements, providing significant reduction of memory requirement and calculation time. Due to its particular formulation, several block calculations can be avoided. Moreover, the junction-to-junction compacting process hidden in the LU process, suggests an intuitive way to label the waves on a network and to reduce the number of fill-in blocks created.

Key words :
Electromagnetic Topology ; Linear Systems ; LU Technique ; Sparse Matrices ; Networks ; Scattering Parameters ; Transmission Lines ; Electromagnetic Compatibility ; Electromagnetic Coupling

* Currently on exchange assignment at Air Force Research Laboratory/DEHP, bldg. 909, 3550 Aberdeen Ave., KAFB NM 87117, USA. This work has been made possible thanks to the Prospective Bureau of DGA and AFOSR.

Intentionally blank

Table of contents

1. Introduction 5
2. Matrix structure of the BLT equation 5
3. Extended application of the BLT equation : subnetwork compacting 8
   3.1. Recalls on the subnetwork compacting process 8
   3.2. Physical significance of generalized scattering parameters 10
      3.2.1. Equivalent scattering parameter significance 10
      3.2.2. Equivalent source wave significance 12
   3.3. Application to electric circuits and transmission-line theory 13
   3.4. Generalization of the BLT equation to the compacting process 14
   3.5. Practical computation improvements 15
4. Taking into account the sparse BLT matrix structure 16
   4.1. Recall of the LU method and its adaptation to a sparse matrix 16
   4.2. Creation of non-initially null-blocks : the fill-in 17
5. Topological analysis of the LU process 18
   5.1. Physical significance of the LU process 18
   5.2. Representing the BLT equation in a graph form 21
      5.2.1. Representing the solution with graphs 21
      5.2.2. Attempt to use classical flow-graph calculation rules 22
      5.2.3. Explanation of the fill-in with graph representation 24
   5.3. The BLT equation as a succession of subnetwork compacting steps 25
6. Labeling waves on a network 27
   6.1. Importance of wave labeling 27
   6.2. Analysis of the fill-in process on elementary networks 28
      6.2.1. Chain-subnetwork 28
      6.2.2. Branch-subnetworks 32
      6.2.3. Loop subnetworks 33
   6.3. Definition of an improved labeling method 33
      6.3.1. The chain-path-march rule 33
      6.3.2. Application on branch-networks 34
      6.3.3. Application on loop networks 36
   6.4. Application : calculation time improvements 37
      6.4.1. General objectives 37
      6.4.2. Number of tube dependence : chain-networks and branch-networks 37
      6.4.3. Example of loop network 41
7. Conclusion 42
References 43

Table of figures

Fig. 2-1 : Fundamental terminology of a topological network 6
Fig. 2-2 : Structure of the $W_{u,v}$ characteristic matrix of [S] supermatrix for a specific set of waves on figure 2-1 network 7
Fig. 3-1 : Terminology of compacted subnetworks 9
Fig. 3-2 : Equivalent network leading to the subnetwork compacting formula 10
Fig. 3-3 : External junction matching applied on figure 3-1 subnetwork 11
for the determination of its equivalent scattering parameters, Seq 11
Fig. 3-4 : Principle of the scattering parameter determination, exciting one port "j" 12
of the equivalent junction 12
Fig 3-5 : Application of the general scattering matrix definition to an electric circuit network 13
Fig. 3-6 : Calculation of the Thevenin's equivalent 14
generator vector on an electric circuit subnetwork 14
Fig. 4-1 : Location of the fill-in and modified blocks in the characteristic matrix of the BLT equation 18
Fig. 5-1 : Labeling of waves and source waves on a single tube 19
Fig. 5-2 : Expression of $W_2(0)$ as an addition of three wave terms, A+B+C 20
Fig. 5-3 : Expression of $W_1(0)$ after the determination of $W_3(0)$ 20
Fig. 5-4 : Flow-graph representation of the propagation and scattering equations on a tube 21
Fig. 5-5 : Different paths for the calculation of $W_2(0)$ with respect to figure 5-4 graph 21
Fig. 5-6 : Different paths for the calculation of $W_1(0)$ on figure 5-4 graph. 22
Fig. 5-7 : Two tube topological network 23
Fig. 5-8 : Graph representation of (5-11) 23
Fig. 5-9 : Representation of the $\Pi_{u,v}$ characteristic matrix of figure 5-7 network 25
Fig. 5-10 : Graph representation of the $\Pi_{u,v}$ characteristic matrices of figure 5-9 graph 25
Fig. 6-1 : Example of linear network with a random labeling 28
Fig. 6-2 : Characteristic matrix of the BLT equation for figure 6-1 network 28
Fig. 6-3 : Graph representation of the BLT equation of figure 6-1 28
Fig. 6-4 : Different reduced graph for figure 6-1 BLT resolution 29
Fig. 6-6 : New labeling of figure 6-1 network 30
Fig. 6-7 : Characteristic matrix of the BLT equation for figure 6-6 network 31
Fig. 6-8 : Graph representation of the BLT equation of figure 6-6 31
Fig. 6-9 : Different reduced graphs for figure 6-6 BLT resolution 31
Fig. 6-10 : Example of a branch-subnetwork with its associated BLT characteristic matrix 32
Fig. 6-11 : Optimized labeling on the branch-subnetwork of figure 6-10 and 32
associated BLT characteristic matrix 32
Fig. 6-12 : Example of a loop network and its associated BLT characteristic matrix 33
Fig. 6-13 : Application of the chain-path-march labeling method on figure 2-1 network 35
Fig. 6-14 : BLT equation characteristic matrix for figure 6-13 network 35
Fig. 6-15 : Example of a loop network requiring tail-path marching and general chain-path marching 36
Fig. 6-16 : Generic chain-subnetwork 38
Fig. 6-17 : Generic branch-subnetwork 38
Fig. 6-18 : Chain-network configuration : computation times for direct and sparse LU resolution compared to tube and junction parameter calculation 39
Fig. 6-19 : Chain-network configuration : calculation time for different sparse LU techniques 39
Fig. 6-20 : Chain-network configuration : fill-in per blocks for 3 labeling methods 39
Fig. 6-21 : Branch-network configuration : computation times for direct and sparse LU resolution compared to tube and junction parameter calculation 40
Fig. 6-22 : Branch-network configuration : calculation time for different sparse LU techniques 40
Fig. 6-23 : Branc-network configuration : fill-in per blocks for 4 labeling methods 40
Table 6-1 : fill-in obtained for figure 6-15 loop network 41
Table 6-2 : calculation times obtained for figure 6-15 loop network 41

1. Introduction

In the past ten years, Electromagnetic topology has moved from the status of a theory ([1], [2]) to the status of an applied technique to predict and control electromagnetic (EM) coupling on large scale systems ([3], [4], [5]). Many efforts have been carried out to demonstrate the power of the method. Most of the calculations have focused to demonstrate the capabilities of the famous BLT equation ([6], [7], [8], [9]). As an example, the CRIPTE code, developed at ONERA since 1990, is now widely considered as a reference in the prediction of EM coupling on large cable networks for Electromagnetic Compatibility (EMC) and Electromagnetic Interaction (EMI) purposes [10]. Of course, many models are still missing to improve the prediction , especially at high frequency. But now, the method is sufficiently mature to allow considering numerical improvements [11]. With the success of the method, people want to treat more and more complex theoretical [12] and applied problems [13], and in addition to the comfort of a computer interface, they require high performance calculations. Even if, with the compacting capability, the method always provides an efficient way to deal with whatever size of systems, the new perspectives of statistical calculations and high frequency modeling would soon require computation means larger than a few years ago, if non-improved numerical techniques keep on being used.

The objective of this paper is to point out the significance and the structure of the BLT equation in order to improve the calculation speed and the memory requirement in EM topology problems. Of course, the straightforward idea will be to use the well-known Gauss LU inversion process [14]. Instead of considering scalars, as usual, the modified algorithm will have to operate on blocks [15]. However, the objective of this paper is not to present a new numerical method. In complement to the numerical aspect, it is considered that the interesting point to emphasize here will be the physical significance hidden under the LU process and its relation to the subnetwork compacting formalism.

Compared to a direct method, acting on the whole BLT matrix, taking into account the existence of zero blocks will always lead to improvements. Moreover, depending on the way the waves are labeled on the network, the computation time and the memory requirement may vary. So additional optimizations, based on the physical significance of the LU process, could be obtained by finding appropriate ways to label the waves.

2. Matrix structure of the BLT equation

This article is not the place to give an exhaustive description of the theory of quantitative EM topology; this has been treated in many references ([1],[2],[3],[4]). Nevertheless, a quick overview of the fundamental equations and fundamental terminology could help for a better understanding of our purpose.

From a general point of view, a topological network is made of ***tubes*** connected to each other by ***junctions*** (figure 2-1). A topological network may represent different parts of a system ; an electrical circuit, the cable wiring, the connections between constitutive physical volumes. The BLT equation is the equation describing the whole coupling on a topological network. Its compacted form is the following (BLT1 form, [1]) :

$$\{[I]-[S]\cdot[\Gamma]\}\cdot[W(0)]=[S]\cdot[Ws] \qquad (2\text{-}1)$$

where :

- [I] is the unit matrix,
- [W(0)] is the unknown ***supervector*** of all the ***outgoing waves*** at the junction level. On each tube, there are two waves propagating from each extremity junction. W(0) is the value of the wave at one end of the tube, according to a given propagation direction. W(0) is a vector itself, which components are the elementary scalar unknowns propagating on a tube (reason of the so-called supervector),
- [Ws] is the ***source wave*** supervector. It contains all the elementary source wave vectors Ws encountered on the network. Ws can be seen as an equivalent source wave obtained at the other end of the tube,

- [Γ] is the ***propagation supermatrix***, relating waves at each extremity of the tube. It is made by the elementary Γ matrices of each tube (reason of the so-called "super" matrix),
- [S] is the ***scattering super matrix***, relating incoming and outgoing waves at each junction. It is made by the elementary scattering parameters of each junction.

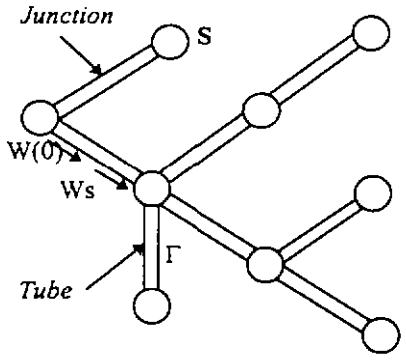

Fig. 2-1 : Fundamental terminology of a topological network

The Γ matrix is particularly interesting when the tube happens to be a ***multiconductor*** transmission line representing a piece of cable harness with homogeneous cross-section. In the case where no propagation has to be considered between junctions (connection of volumes for instance), the length of the tube is said to be ***shrunk to zero*** and the Γ matrix becomes equal to the unit matrix. The BLT equation is then written in the so-called BLT2 form [1]. To keep this presentation its generality, we will always consider non-zero length tubes with non-unit Γ matrices.

[Γ] and [S] supermatrices have a specific elementary block structure. For both matrices, the allocation of the non-zero blocks is given by the so-called ***"characteristic matrices"***. Those matrices are defined as a function of the wave numbers. The presence of a "0" coefficient or a "1" coefficient indicates whether the block is null or not. The structure of the [Γ] supermatrix is quite obvious. It is a block diagonal matrix. The diagonal blocks are equal to the propagation matrix of each tube. So the characteristic matrix of [Γ] is nothing more than the unit matrix.

The structure of the [S] supermatrix, $W_{u,v}$, is less obvious. This matrix has to relate the outgoing waves to the incoming waves at each junction. So the [S] supermatrix is not directly built by introducing the elementary junction scattering parameter matrices of each junction as diagonal blocks. Those elementary matrices have to be split with respect to the wave on which they apply. In this case, the use of the $W_{u,v}$ characteristic matrix proves itself to be of great interest. The definition of this matrix is the following :

- $W_{u,v} = 0$, if there is no junction J into which the W_v wave comes, and the W_u wave leaves,
- $W_{u,v} = 1$, if there is a junction J into which the W_v wave comes, and the W_u wave leaves

Figure 2-2 gives an example of the $W_{u,v}$ matrix for the set of waves on figure 2-1 network. One will notice that for a total of 16x16=256 blocks constituting the [S] supermatrix, only 38 blocks are non-zero. We can say that the matrix is filled at 15 % only. The important point to keep in mind is that the structure of the [S] matrix would change with a new set of labeled waves, but the number of initially non-zero blocks would remain the same.

From a computational point of view, it is obvious that only the non-zero blocks have to be stored in memory. As an example, in the CRIPTE code, the Γ matrix is stored for each tube but the entire $[\Gamma]$ supermatrix is never loaded in memory. Identically, for each junction, the S matrix is calculated, and then each $S_{u,v}$ non-zero block is stored in a table. The location of the beginning of each non-zero block is referenced thanks to a data allocation pointer and the knowledge of the $W_{u,v}$ characteristic matrix.

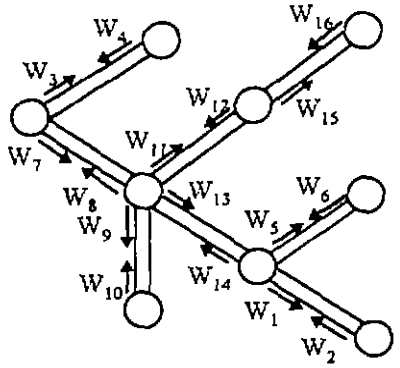

$$W_{u,v}=\begin{pmatrix}
0&1&0&0&0&0&0&0&0&0&0&0&0&0&0&0\\
1&0&0&0&0&1&0&0&0&0&0&0&1&0&0&0\\
0&0&0&1&0&0&0&1&0&0&0&0&0&0&0&0\\
0&0&1&0&0&0&0&0&0&0&0&0&0&0&0&0\\
1&0&0&0&0&1&0&0&0&0&0&0&1&0&0&0\\
0&0&0&0&1&0&0&0&0&0&0&0&0&0&0&0\\
0&0&0&1&0&0&0&1&0&0&0&0&0&0&0&0\\
0&0&0&0&0&0&1&0&0&1&0&1&0&1&0&0\\
0&0&0&0&0&0&1&0&0&1&0&1&0&1&0&0\\
0&0&0&0&0&0&0&0&1&0&0&0&0&0&0&0\\
0&0&0&0&0&0&1&0&0&1&0&1&0&1&0&0\\
0&0&0&0&0&0&0&0&0&0&1&0&0&0&0&1\\
0&0&0&0&0&0&1&0&0&1&0&1&0&1&0&0\\
1&0&0&0&0&1&0&0&0&0&0&0&1&0&0&0\\
0&0&0&0&0&0&0&0&0&0&1&0&0&0&0&1\\
0&0&0&0&0&0&0&0&0&0&0&0&0&0&1&0
\end{pmatrix}$$

Fig. 2-2 : Structure of the $W_{u,v}$ characteristic matrix of [S] supermatrix for a specific set of waves on figure 2-1 network

The resolution of the BLT equation is equivalent to the resolution of the following linear equation :

$$A \cdot X = B \tag{2-2}$$

where :

- $A = [I] - [S][\Gamma]$, the sparse matrix to invert,
- $B = [S][Ws]$, the second member vector of the linear equation,
- $X = [W(0)]$, the vector of the unknown outgoing waves.

Because $[\Gamma]$ is block diagonal, the structure of A is very close to [S] one. The only difference is that it contains unit blocks on the diagonal. We call $\Pi_{u,v}$ the characteristic matrix of A, or ***the characteristic matrix of the BLT equation***. We can notice that :

$$\Pi_{u,v} = [I_{u,u}] + W_{u,v} \tag{2-3}$$

where $I_{u,u}$ represents the unit matrix referred to a W_u wave.

If we take the example of the network presented on figure 2-2, the characteristic matrix of the BLT equation shows that the matrix used for the calculation is filled at 20% of the total number of blocks only. A direct resolution method like a LU inversion process would require one to load the whole matrix in memory. Although the individual storage of $[\Gamma]$ and [S] matrices was already made by blocks, this direct resolution method was however the one used in the CRIPTE code until this time.

3. Extended application of the BLT equation : subnetwork compacting

3.1. Recalls on the subnetwork compacting process

The success of the BLT equation does not come from the fact that it was the first network equation ever published. Network theory for lumped elements was known since a long time before the publication of the BLT equation [2]. A long time ago, network theory had been already applied, especially for circuit networks [16]. These network equations were mainly based on the impedance matrix, Z ,or admittance matrix, Y, calculations. In the past few years, it has been generalized to Electromagnetic Scattering theory [17]. However, compared to the classical network methods, the specificity of the BLT equation lies on the use of scattering matrices which provides two main advantages :

- scattering parameters are always defined, which is not always the case for Z and Y parameters,
- scattering parameters, associated to the propagation matrix, give the BLT equation its generality, because they allow its direct application to any kind of network problem. This way, the BLT equation is perfectly matched for EM topology purpose.

Moreover, an other interest of the BLT equation formalism has also been pointed out in the recent few years : ***network compacting*** ([4], [18]). According to the sub-problem decomposition process on which EM topology theory is based, this operation deals with treating a part of network called ***subnetwork***, in an equivalent form, closely related to a generalized Thevenin's model [16]. The equivalent topological model is made of two quantities :

- an equivalent junction, characterized by its scattering parameters, $S_{eq.}$
- a set of equivalent sources applied at each equivalent junction port, characterized by an equivalent source wave vector, $Ws_{eq.}$

The interest in the compacting lies on the fact that the equivalent junction and its associated equivalent sources can be used in other networks, with different topologies. This feature opens EM topology to a wide variety of applications :

- the treatment of any size of problem by decomposing it in subnetworks, allowing calculation on small computers [9],
- the treatment of non linear junctions, applying a time domain convolution [19],
- the transformation of a network computation code into a *multiple channel* numerical network analyzer [18],
- the modeling of inverse problems such as Electromagnetic Compatibility noise source determination with an LISN device [20], or the determination of distributed generators on a test wiring [13].

Figure 3-1 presents the terminology of subnetworks. A subnetwork is made of ***internal junctions***. Tubes connecting two internal junctions are called ***internal tubes***. Tubes connected to ***external junctions*** are called ***external tubes***. The elementary ends of the tubes, at the external junction levels, are called ***ports*** as for classical junctions. The figure shows the associated equivalent network when the equivalent junction is used. On both networks external tubes 1, 2, 3 and external junctions 1, 2,3 identical. On each of the external tubes "i", equivalent source wave vectors Ws_{eqi}, representing the possible existence of sources inside the subnetwork, are applied.

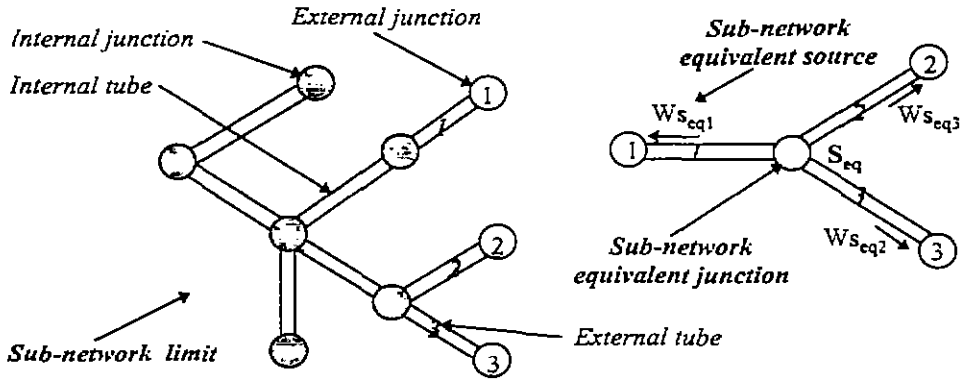

Fig. 3-1 : Terminology of compacted subnetworks

In [18], it has been shown that equivalent scattering parameters could be calculated applying a topological reduction of any subnetwork of the original configuration, called "network A", in a "*rattle*" equivalent network (figure 3-2), involving a "***self tube***" [2]. W_I and W_{II} are the supervector waves propagating on the equivalent external tube. This tube is characterized by the Γ_I propagation supermatrix, made by all the elementary propagation matrices of all the external tubes. The same definitions are applied for W_{III} and Γ_{III} but for internal tubes. $S_{I,II}$ is the scattering parameter supermatrix made by all the elementary scattering parameter matrices of the external junctions. Same definition is applied for S_{int} but for internal junctions. The elimination of W_{III} in the rattle network leads to the identification of W_I and W_{II} waves obtained on network A with the ones defined on a network where internal equivalent tubes are removed, called "network B". So one obtains the derivation of the scattering parameter matrix, S_{eq}, equivalent to the subnetwork.

$$S_{eq} = S_{I,II} + S_{II,III} \cdot \Gamma_{III} \cdot \left(1 - S_{III,III} \cdot \Gamma_{III}\right)^{-1} \cdot S_{III,II} \tag{3-1}$$

In (3-1), the only difference with the expression given in [18] is that we do not take into account the external tubes in the compacting. The fact of including the external tubes in the relation is simply made by multiplying (3-1), on the right and on the left, by Γ_I.

It is also interesting to calculate the equivalent source waves obtained when internal sources Ws_{III} exist in the subnetwork, in addition to Ws_I and Ws_{II} source waves on the external tube. Now, the identification of the two BLT equations for network A and network B gives the value of Ws_{eqI} and Ws_{eqII} .

BLT equation for network A :

$$\begin{pmatrix} 1 & -S_{I,II} \cdot \Gamma_I & 0 \\ -S_{II,I} \cdot \Gamma_I & 1 & -S_{II,III} \cdot \Gamma_{III} \\ -S_{III,I} \cdot \Gamma_I & 0 & 1 - S_{III,III} \cdot \Gamma_{III} \end{pmatrix} \cdot \begin{pmatrix} W_I \\ W_{II} \\ W_{III} \end{pmatrix} = \begin{pmatrix} S_{I,II} \cdot Ws_{II} \\ S_{II,I} \cdot Ws_I + S_{II,III} \cdot Ws_{III} \\ S_{III,I} \cdot Ws_I + S_{III,III} \cdot Ws_{III} \end{pmatrix} \tag{3-2}$$

BLT equation for network B :

$$\begin{pmatrix} 1 & -S_{I,II} \cdot \Gamma_I \\ -S_{eq} \cdot \Gamma_I & 1 \end{pmatrix} \cdot \begin{pmatrix} W_I \\ W_{II} \end{pmatrix} = \begin{pmatrix} S_{I,II} \cdot Ws_{eqII} \\ S_{eq} \cdot Ws_{eqI} \end{pmatrix} \tag{3-3}$$

The two first equations of (3-2) and (3-3) give a direct identification of Ws_{eqII} :

$$Ws_{eqII} = Ws_{II} \tag{3-4}$$

The interesting result of (3-4) is that the compacting does not produce any more wave source term, with respect to W_{II} propagation direction.

The elimination of W_{III} in the third equation of (3-3) gives the expression of Ws_{eqI} :

$$Ws_{eq_I} = Ws_I + S_{eq}^{-1} \cdot \left(S_{II,III} \cdot Ws_{III} + S_{II,III} \cdot \Gamma_{III} \cdot \left(1 - S_{III,III} \cdot \Gamma_{III}\right)^{-1} \cdot S_{III,III} \right) \cdot Ws_{III} \tag{3-5}$$

(3-5) shows that the compacting operation produces an additional source wave term which is added to the original one, Ws_I. From a computation point of view, this relation reveals itself to be complicated because it involves the calculation of the inverse of S_{eq} block matrix. This is the reason why, when demonstrated in [18], no existing source had been considered on the internal tubes. Generally, as we will see later, Thevenin's equivalent model, although involving two equivalent source waves, is much more simple for the compacting applications than (3-5) equivalent source expression.

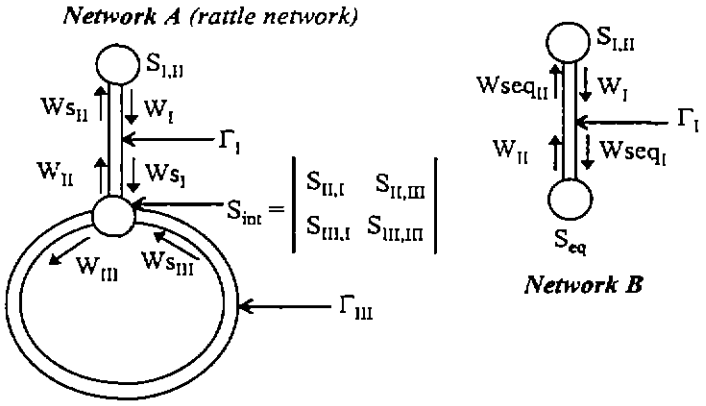

Fig. 3-2 : Equivalent network leading to the subnetwork compacting formula

3.2. Physical significance of generalized scattering parameters

3.2.1. Equivalent scattering parameter significance

In the BLT equation, according to the topological network theory, scattering parameters are referenced to a normalizing impedance matrix [Zc]. If no propagation is considered in the network (Γ = I), any value of [Zc] can be chosen. For instance, the value can be chosen equal to a scalar (typically $[Zc] = R_o.[I]$, with $R_o = 50\ \Omega$). In the particular case where the network is a transmission-line network, [Zc] has to be equal to the characteristic impedance made by all the characteristic impedance matrices of the tubes connected to the junction [2]. However, in all the cases, a general definition of the scattering matrix [S] at a junction can be given without mentioning explicitly a normalizing [Zc] matrix. Indeed, it can be said that a scattering parameter matrix [S] relates an outgoing wave vector [W^-] to an incoming wave vector [W^+] ([21], [22]).

$$[W^-] = [S].[W^+] \tag{3-6}$$

(3-6) is nothing but a matrix generalization of the well-known reflection coefficient definition. The S_{ij} terms of the [S] matrix will thus be equal to the ratio of the outgoing wave at port "i" to the incoming wave at port "j", when all the incoming wave at port k≠j is made equal to 0 :

$$S_{ij} = \left.\frac{W_i^-}{W_j^+}\right|_{W_{k\neq j}^+ = 0} \tag{3-7}$$

(3-7) suggests another way to calculate all the scattering parameters on a subnetwork, different from the one described in section 3.1, and more closely related to a direct BLT formulation. Effectively, all the incoming waves in the junction can be made equal to zero by loading each tube connected to the junction by a load which scattering parameters are equal to 0 (matched load). Figure 3-3 gives an example for the determination of the scattering parameters of the subnetwork presented on figure 3-1.

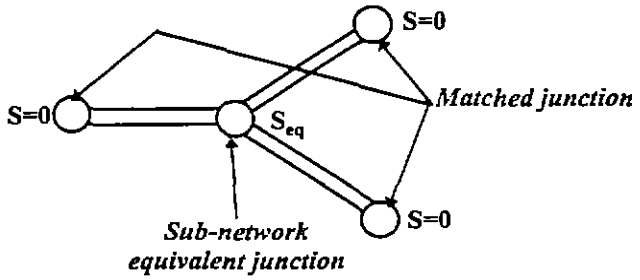

Fig. 3-3 : External junction matching applied on figure 3-1 subnetwork for the determination of its equivalent scattering parameters, Seq

Figure 3-4 gives another representation of the figure 3-3 equivalent problem, directly derived from network B representation (figure 3-2). We suppose that the length of the external tubes is taken equal to zero because we are only interested in what happens at the equivalent junction port level. As figure 3-2, two waves are defined on the tube :

- W_I, directed towards the subnetwork equivalent junction, and
- W_{II}, directed towards the equivalent external junction.

Now, let us suppose that the port "j" is excited by a localized asymmetric source, chosen equal to "1" to simplify our problem. The source definition depends on the definition of the waves used on the tube. For example, if the waves are defined as a combination of EM fields, the asymmetric source will be an electric field. If the waves are defined as a combination of voltages and currents, the anti-symmetric source can be a voltage generator. As seen in section 3.1, this physical source applied on an external tube gives birth to two source wave vectors, Ws_{eqI} and Ws_{eqII} (there is no source on the internal tubes). Because the length of the tube is zero, the two source waves have the same amplitude and opposite signs. So, on any port "i" of the equivalent junction, the incoming and outgoing waves are given by :

$$W_i^+ = W_{I,i}(L) = W_{I,i}(0) + Ws_{eq_{I,i}} = Ws_{eq_{I,i}} \tag{3-8}$$

$$W_i^- = W_{II,i}(0) = W_{II,i}(L) - Ws_{II,i} = W_{II,i}(L) + Ws_{I,i} \tag{3-9}$$

where, $W_{II,i}$, $W_{I,i}$, $Ws_{II,i}$, $Ws_{I,i}$ are the i^{th} components of "I" and "II" waves and source waves. It is important to mention that, even if the length of the tubes involved in this calculation is zero, we introduced a generic length "L". The reader must imagine that L is very small. This way is convenient to point out the distinction between the wave values at both ends of the tube when a source is applied on it. In our case, for one given configuration, only the j^{th} component of these vectors is non-zero. Consequently, the definition

of the scattering parameters between two ports "j" (injection port) and "i" (reception port) becomes obvious. Considering whether "i" is equal to "j" or not. We can write :

$$S_{ij} = \frac{W_i^-}{Ws_{I,j}} = W_{II,i}(L)\,, \quad \text{for } i \neq j \tag{3-10}$$

$$S_{jj} = \frac{W_{II,j}^-}{Ws_{I,j}} = \frac{Ws_{I,j} + W_{II,j}(L)}{Ws_{I,j}} = 1 + W_{II,j}(L) \tag{3-11}$$

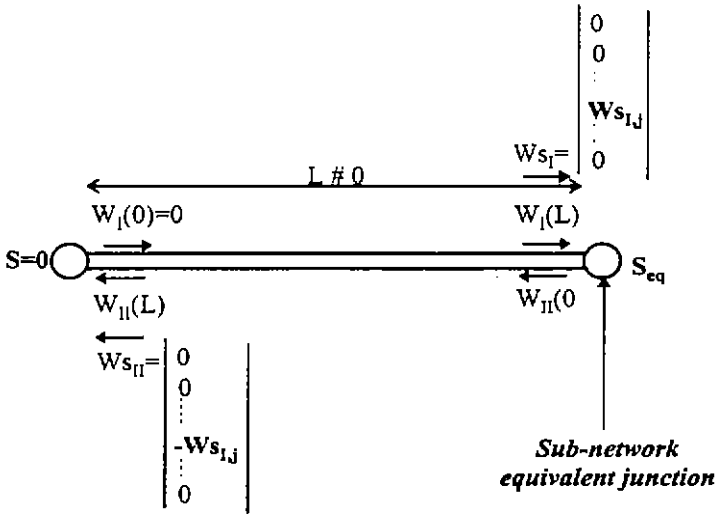

Fig. 3-4 : Principle of the scattering parameter determination, exciting one port "j" of the equivalent junction

3.2.2. Equivalent source wave significance

In section 3.1, (3-5) shows that, if there is no external source wave, only a Ws_{eqI} source wave is created in the compacting process. Meanwhile, no source wave Ws_{eqII} is created in the opposite direction. We also mentioned that this relation is not really very convenient for computational aspects. Hopefully, according to the generalization of Thevenin's equivalent theorem, the presence of physical sources inside the subnetwork can also be summarized in a more simple way by the application of a localized asymmetric voltage source vector, E_{eq}, going out at each port of the equivalent junction. Consequently, as in section 3.2.1, two source waves will have to be defined. Using the general definition of source wave vector [2], we find :

$$Ws_{eq_I} = -\int_0^L e^{-(L-z)\gamma} E_{eq} . \delta(L-z) . dz = E_{eq} \tag{3-12}$$

$$Ws_{eq_{II}} = +\int_0^L e^{-(L-z)\gamma} E_{eq} . \delta(z) . dz = -E_{eq} = -Ws_{eq_I} \tag{3-13}$$

Meanwhile, according to figure 3-4 definitions, the following propagation and scattering relations are available :

$$W_{II}(L) = W_{II}(0) + Ws_{eqII} \tag{3-14}$$

$$W_I(L) = -Ws_{eqII} \tag{3-15}$$

$$W_{II}(0) = S_{eq} . W_I(L) \tag{3-16}$$

$W_{II}(L)$ is directly accessible on the real subnetwork (it could be measured in an experiment). Eliminating $W_I(L)$ and $W_{II}(0)$ in (3-15) and (3-16), and reporting in (3-14), we obtain :

$$Ws_{eqII} = (1 - S_{eq})^{-1} W_{II}(L) \tag{3-17}$$

3.3. Application to electric circuits and transmission-line theory

As an application, it is interesting to see how (3-6), (3-7) and (3-13) can be applied in the case of electric circuits and transmission-line networks. In this case, outgoing and incoming waves will be expressed as a combination of an input voltage vector [V], and an input current vector [I] :

$$[W^-] = [V] - [Zc]\,[I] \tag{3-18}$$

$$[W^+] = [V] + [Zc]\,[I] \tag{3-19}$$

and (3-2) takes the following form :

$$([V] - [Zc]\,[I]) = [S]\,([V] + [Zc]\,[I]) \tag{3-20}$$

Matching the external junctions of the subnetwork is made by loading each tube connected to the junction by a load whose impedance matrix is equal to the characteristic impedance of each tube (figure 3-5). When exciting each port "j" by a voltage generator E_j, the application of (3-10) and (3-11) gives :

$$S_{ij} = \frac{2V_i}{E_j} \qquad \text{for } i \neq j \tag{3-21}$$

$$S_{jj} = \frac{2V_j}{E_j} + 1 \tag{3-22}$$

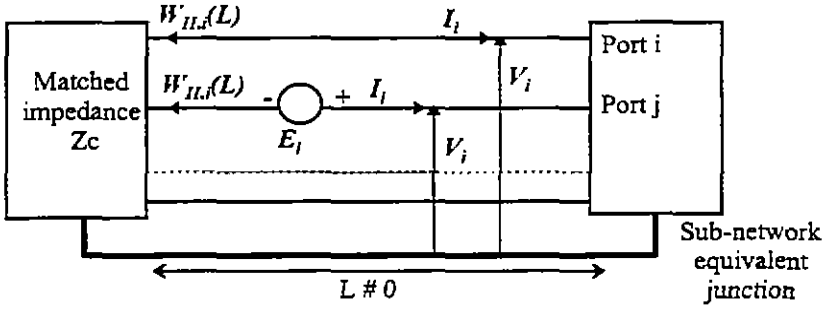

Fig. 3-5 : Application of the general scattering matrix definition to an electric circuit network

We find the result well known by people used to run network analyzers in experiments. Between two different ports, a scattering parameter is equal to two times the gain between the output voltage and the input generator. But, on the same port, the scattering parameter is equal to "1" plus the same gain [21].

For the determination of the Thevenin's equivalent generator voltage vector, E_{eq}, it is possible to derive a circuit scheme similar to the one we derived on figure 3-5 (figure 3-6). E_{eq} can also be seen as the voltage obtained if the ports of the subnetwork were loaded with open circuits. Z_{eq} is the impedance matrix obtained from the S_{eq} scattering matrix [4] :

$$Z = (1 - S_{eq})^{-1}.(1 + S_{eq}).Zc \tag{3-23}$$

Knowing the output voltage on the Zc load, Vs, (calculated with a BLT resolution), we obtain the value of E_{eq} :

$$E_{eq} = (Z_{eq}.Zc^{-1}-1).Vs = [(1 - S_{eq})^{-1}(1 + S_{eq}) + 1]\,Vs = 2\,(1 - S_{eq})^{-1}\,Vs \tag{3-24}$$

If we had taken (3-17) instead of applying electric configurations, $W_{II}(L) = 2\,Vs$ (because the external equivalent junction is matched) would have given the same result.

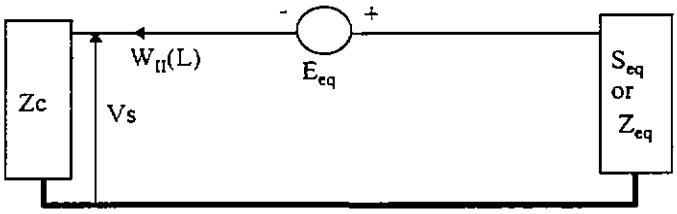

Fig. 3-6 : Calculation of the Thevenin's equivalent generator vector on an electric circuit subnetwork

3.4. Generalization of the BLT equation to the compacting process

The problem with (3-1) is that the compacting resolution technique is not really a BLT equation resolution. From a computation point of view, it would be suitable to have the same subroutine for the resolution of the BLT equation on a total network and for the calculation of the equivalent model on a subnetwork. Equations (3-10), (3-11) and (3-17) demonstrate that it is possible to calculate the equivalent scattering matrix, S_{eq}, and the equivalent source wave vector, Ws_{eq}, by solving several BLT equations on different configurations, dealing with specific source excitations on each port of the subnetwork. All those configurations are obtained by virtually "disconnecting" the subnetwork from the rest of the network and by loading each external tube by a matched junction.

Now, from a numerical point of view, we must remember that the resolution of a BLT equation is nothing more than the resolution of a linear system. Consequently, in (1-1), it is easy to replace the [Ws] supervector by a NxM $[Ws_g]$ generalized super-matrix. $[Ws_g]$ is made by the assembling of different $[Ws_k]$ supervectors, k being a k^{th} source configuration applied on the network and M the total number of source configurations). By this way, we obtain a generalization of the BLT equation to a ***multiple source state*** second member.

$$\{[1] - [S]\cdot[\Gamma]\}\cdot[W(0)] = [S]\cdot\left\{Ws_g\right\} \tag{3-25}$$

with :

$$\left\{Ws_g\right\} = \left\{\left[Ws_1\right]\ \left[Ws_1\right]\ \cdots\ \left[Ws_M\right]\right\} \tag{3-26}$$

In the particular case of the compacting problem, the elementary $[Ws_k]$ supervectors are associated with the excitation of one given port of the subnetwork by an elementary localized source. Moreover, the calculation of the equivalent source vector can be calculated in the same way because it can be achieved by the same load configuration as the one used for the subnetwork scattering parameter determination. In this case the supervector is made by the application of the actual sources existing inside the subnetwork limits. So, if the number of ports of the subnetwork is M, the second member matrix will have a 2Mx(M+1) size in the multiple source state BLT equation.

In the future, the multiple state source BLT equation will certainly have further applications, especially for the treatment of inverse problems. It will be particularly suitable in the so-called ***test wiring*** method, in which, thanks to the knowledge of the response of a wire to elementary distributed sources, it is possible to come back to the actual voltage generators of the transmission-line model [13].

3.5. Practical computation improvements

As we saw in the previous section, the interest in a multiple state generalized BLT equation relies on the fact that the same numerical method can be applied to solve a classical BLT equation problem or a subnetwork compacting problem.

As an example of the computation improvement, we can mention how convenient such a calculation has become in the CRIPTE code. Before, either the BLT equation resolution, the calculation of subnetwork scattering parameters, or the Thevenin's generator determination requested respectively three different calculations :

- *the resolution of a linear system (BLT equation),*
- the computation of (3-1), involving multiple matrix block inversion (compacting equation),
- the resolution of a linear system on the subnetwork when all the external junctions were open circuits (BLT equation).

Nowadays, in the CRIPTE code, all the network calculations are based on the same numerical subroutine. Depending on the user's choice, the classical BLT calculation can be made on the total network or the compacting calculation. In this case, the calculation of the equivalent scattering parameter matrix and the calculation equivalent Thevenin's generator vector can be achieved on the subnetwork. The scattering parameter calculation is always performed, because they are required in the equivalent source definition. But, if there is no source inside the subnetwork, the equivalent source calculation is not performed.

In addition, this method is also interesting for the significant memory improvement it provides. Indeed, (3-1) requires the declaration of several matrix blocks, whereas they are less numerous for the multiple state BLT equation.

4. Taking into account the sparse BLT matrix structure

4.1. Recall of the LU method and its adaptation to a sparse matrix

As we pointed out in the previous section, the "A" matrix to invert in the BLT equation (3-2) is widely sparse. The location of the zero blocks is not random, but imposed by the topology of the network. Moreover, this topology leads to a block structure in which zero values and non-zero values are gathered in blocks. So it is natural to think of applying a Gauss linear system process by acting on the matrix blocks instead of acting on the scalar components of the BLT matrix. Let us recall the general method of a Gauss inversion process or so-called ***LU process***. The first step is to organize the system to solve as a triangle system. Then, beginning from the lower side of the triangle the solution of the system is found easily by climbing up the triangle.

Let us consider A, the NxN matrix to be inverted and B, an NxNsecm second member matrix. N is the size of the matrix and Nsecm is the number of second member column vectors. We can propose the very simple algorithm written:

```
# Do for I = 1 , N-1
    # Do for J = I+1 , N
        # If A(J,I) ≠ 0 then
            coef = A(J,I)/A(I,I)
            # Do for K = I+1 , N
                A(J,K) = A(J,K) - A(I,K)*coef                    (4-1)
            End do #
            # Do for K =1 , Nsecm
                B(J,K) = B(J,K) + B(J,K)*coef
            End do #
        End if #
    End do #
End do #
```

Of course, in this simple algorithm, we suppose here that A(I,I) terms are all non-zero. It is well known that more algorithms are based on the search for the best ***pivot*** and that many numerical methods are available to optimize the computation time and memory requirement. In our case, this straightforward algorithm will find a direct utility when the "A" matrix is block constituted. Consequently, (4-1), let us remove all the brackets and now think an "$A_{I,J}$" coefficient in terms of a matrix block instead of a scalar. Let us consider that N is now the number of blocks. The scalar coefficient "coeff" becomes a matrix block "$COEFF_{I,I}$". The algorithm becomes the following :

```
# Do for I = 1 , N-1
    # Do for J = I+1 , N
        # If A_J,I ≠ 0 then
            COEFF_I,I = A_J,I *A_I,I^-1
            # If A_I,K ≠ 0 then
                # Do for K = I+1 , N
                    A_J,K = A_J,K - COEFF_I,K *A_J,K             (4-2)
                end do #
            End if #
            # Do for K =1 , Nsecm
                B_J,K = B_J,K + COEFF_I,K *B_J,K
            End do #
        End if #
    End do #
End do #
```

The interesting point of (4-2) is that the $A_{i,j}$ block is generally non zero. Indeed, as seen in (2-1), the diagonal blocks of the BLT matrix are unit matrices. Even modified by the "*triangularization*" process, the chance to obtain a zero block is quite null.

Compared to the previous scalar algorithm, all the interest of this block algorithm deals in the "# If $A_{J,I} \neq 0$" and "# If $A_{I,K} \neq 0$" conditions. Indeed, if these conditions are verified on a matrix block, a whole set of operations can be avoided. The number of operations is much smaller than the one for the direct method on the whole matrix ($\frac{N(N-1)(2N+5)}{6}$ operations # N^3, when N is large). For the sparse inversion process, because the number of operations depends on the number and the location of non-zero blocks, it is difficult to give a similar formula.

4.2. Creation of non-initially null-blocks : the fill-in

Looking at the matrix block Gauss algorithm for a sparse matrix (4-2), one will notice that some blocks, initially equal to zero in the matrix can become non-zero. Let us suppose that we are at the step "i" of the triangularization process with $A_{I,I}$ as the pivot block. Such a modification of the matrix structure may occur on an $A_{K,L}$ block, if $A_{I,L}$ and $A_{K,I}$ are non-zero blocks as well. This modification is called ***fill-in***. By extension, we will call fill-in number, the number of newly created non-zero blocks. We will also call *fill-in* this number.

At the step "i" of the process, considering an $A_{I,I}$ block pivot, with K>I and J>I, three conditions have to be satisfied at the same time to have a fill-in on an $A_{K,L}$ block :

1) $A_{K,L}$ has to be a originally zero block,
2) $A_{I,L}$ has to be a non-zero block,
3) $A_{K,I}$ has to be a non-zero block.

It has to be noticed that, in the process of fill-in affectation, the newly created non-zero blocks can *themselves participate to the creation of other fill-in blocks.*

Before the calculation, the fill-in allocation can be easily determined considering the $\Pi_{u,v}$ characteristic matrix of the BLT equation (see section 2.). This way, the number of blocks to be stored in can be determined in advance, before the calculation. The important point to notice is that the fill-in number varies as a function of the labeling of the network. Figure 4-1 gives an example of the fill-in allocation for the network described on figure 2-2. One will notice that the diagonal terms are non-zero with respect to the structure of the BLT equation matrix. The fill-in blocs are written "x". The number of fill-in blocks is equal to 14. The total number of non-zero blocs is now equal to 68. The matrix is still 26% filled only.

The initially non-zero diagonal blocks, modified during the process, are denoted by "$\mathcal{I}$". Effectively, as we mentioned, the structure of the BLT equation matrix presents unit terms on the diagonal. So, if a diagonal term is not modified by the process, it remains equal to a unit matrix. Consequently, its inversion and the multiplication by the $A_{I,I}$ block are not required anymore. So other calculations can be avoided. In figure 4-1, 8 diagonal blocks are not modified. The condition for a non modification of a diagonal block $A_{I,I}$ is the following :

1) I=1 : this condition is always verified and this term always remains equal to a unit block,
or
2) for K<I<1, $A_{I,K}$ or $A_{K,I}$ are non-zero blocks. If $A_{K,I}$ and $A_{I,K}$ are non-zero blocks as well, $A_{I,I}$ is modified in the process.

Whenever it is possible, one will have interest to choose a first labeled wave on a "big" tube, made of many components.

$$\Pi_{u,v=}\begin{pmatrix}
1 & 1 & 0 & 0 & 0 & 0 & 0 & 0 & 0 & 0 & 0 & 0 & 0 & 0 & 0 & 0 \\
1 & \underline{1} & 0 & 0 & 0 & 1 & 0 & 0 & 0 & 0 & 0 & 0 & 1 & 0 & 0 & 0 \\
0 & 0 & 1 & 1 & 0 & 0 & 0 & 1 & 0 & 0 & 0 & 0 & 0 & 0 & 0 & 0 \\
0 & 0 & 1 & \underline{1} & 0 & 0 & 0 & x & 0 & 0 & 0 & 0 & 0 & 0 & 0 & 0 \\
1 & x & 0 & 0 & 1 & 1 & 0 & 0 & 0 & 0 & 0 & 0 & 1 & 0 & 0 & 0 \\
0 & 0 & 0 & 0 & 1 & \underline{1} & 0 & 0 & 0 & 0 & 0 & 0 & x & 0 & 0 & 0 \\
0 & 0 & 0 & 1 & 0 & 0 & 1 & 1 & 0 & 0 & 0 & 0 & 0 & 0 & 0 & 0 \\
0 & 0 & 0 & 0 & 0 & 0 & 1 & \underline{1} & 0 & 1 & 0 & 1 & 0 & 1 & 0 & 0 \\
0 & 0 & 0 & 0 & 0 & 0 & 1 & x & 1 & 1 & 0 & 1 & 0 & 1 & 0 & 0 \\
0 & 0 & 0 & 0 & 0 & 0 & 0 & 0 & 1 & \underline{1} & 0 & x & 0 & x & 0 & 0 \\
0 & 0 & 0 & 0 & 0 & 0 & 1 & x & 0 & 1 & 1 & 1 & 0 & 1 & 0 & 0 \\
0 & 0 & 0 & 0 & 0 & 0 & 0 & 0 & 0 & 0 & 1 & \underline{1} & 0 & x & 0 & 1 \\
0 & 0 & 0 & 0 & 0 & 0 & 1 & x & 0 & 1 & 0 & 1 & 1 & 1 & 0 & x \\
1 & x & 0 & 0 & 0 & 1 & 0 & 0 & 0 & 0 & 0 & 0 & 1 & \underline{1} & 0 & x \\
0 & 0 & 0 & 0 & 0 & 0 & 0 & 0 & 0 & 0 & 1 & x & 0 & x & 1 & 1 \\
0 & 0 & 0 & 0 & 0 & 0 & 0 & 0 & 0 & 0 & 0 & 0 & 0 & 0 & 1 & \underline{1}
\end{pmatrix}$$

Fig. 4-1 : Location of the fill-in and modified blocks in the characteristic matrix of the BLT equation

5. Topological analysis of the LU process

5.1. Physical significance of the LU process

From the numerical point of view, the LU process expresses one unknown of the problem as a function of a second member, by deriving an equation in which all the other unknowns have disappeared. From a physical point of view, it is interesting to analyze the result obtained analytically. Of course, in the general case, the equations can become very complex. To simplify the explanation, we will take a single tube network (figure 5-1).

If we consider two waves, W_1 and W_2 propagating in opposite directions on the tube, the ***propagation equation*** for both waves can be expressed as :

$$W_i(L) = \Gamma.W_i(0) + Ws_i \tag{5-1}$$

(5-1) means that $W_i(L)$, the value of the wave at the other end of the tube, can be decomposed in two parts :

- $\Gamma.W_i(0)$: the wave at the origin of the tube when it has propagated on the tube, on a length "L" (multiplication by Γ matrix, providing a delay),
- Ws_i, the equivalent source wave seen at the opposite end of the tube. As an example, if the tube is a multiconductor transmission line, the source wave can be written :

$$Ws_i = \int_0^L e^{-(L-z)\gamma}\left[(Vs(z) + Zc.Is(z)\right].dz \tag{5-2}$$

where : Vs(z) and Is(z) are respectively the per unit length serial voltage and parallel current generators distributed all along the tube. γ is the propagation factor matrix. The meaning of (5-2) is that the equivalent source wave is equal to the collection (integral summation) of all the elementary source waves at the "z"

position (Vs(z) + Zc.Is(z)), taking into account for each of them the phase delay between position L and position z ((L-z).γ).

In figure 5-1, S_{12} and S_{21} represent the scattering parameter matrices of the two terminal junctions. Both of these matrices obey the following ***scattering equation*** :

$$W_i(0) = S_{ij}.W_j(L) \tag{5-3}$$

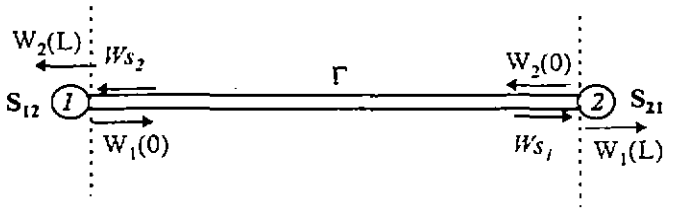

Fig. 5-1 : Labeling of waves and source waves on a single tube

The different steps of the triangularization of the BLT equation, applied on this one tube system are summarized in (5-4) and (5-5) :

$$\begin{pmatrix} 1 & -S_{12}\cdot\Gamma \\ -S_{21}\cdot\Gamma & 1 \end{pmatrix}\cdot\begin{pmatrix} W_1(0) \\ W_2(0) \end{pmatrix} = \begin{pmatrix} 0 & S_{12} \\ S_{21} & 0 \end{pmatrix}\begin{pmatrix} Ws_1 \\ Ws_2 \end{pmatrix} = \begin{pmatrix} S_{12}\cdot Ws_2 \\ S_{21}\cdot Ws_1 \end{pmatrix} \tag{5-4}$$

$$\begin{pmatrix} 1 & -S_{12}\cdot\Gamma \\ 0 & 1-S_{21}\cdot\Gamma\cdot S_{12}\cdot\Gamma \end{pmatrix}\cdot\begin{pmatrix} W_1(0) \\ W_2(0) \end{pmatrix} = \begin{pmatrix} S_{12}\cdot Ws_2 \\ S_{21}\cdot Ws_1 + S_{21}\cdot\Gamma\cdot S_{12}\cdot Ws_2 \end{pmatrix} \tag{5-5}$$

The second equation of (5-5) can also be written :

$$W_2(0) = S_{21}\,\Gamma\,S_{12}\,\Gamma\,W_2(0) + S_{21}\,Ws_1 + S_{21}\,\Gamma\,S_{12}\,\Gamma\,Ws_2 \tag{5-6}$$

This means that the W_2, wave at position 0, is equal to the summation of the three following terms, represented on figure 5-2 :

1 - a wave $A = S_{21}.\Gamma.S_{12}.\Gamma.W_2(0)$: the same wave $W_2(0)$, having propagated along the tube direction (multiplication by Γ), having been reflected on junction 1 (multiplication by S_{12}), having propagated in the other direction (multiplication by Γ) and finally, having been reflected on junction 2 (multiplication by S_{21}),

2 - a source wave $B = S_{21}.Ws_1$: the source wave 1 in the opposite propagation direction, reflected on junction 2 (multiplication by S_{21}),

3 - a source wave $C = S_{21}.\Gamma.S_{12}.Ws_2$: the source wave 2 having been reflected on junction 1 (multiplication by S_{12}), having propagated on the tube (multiplication by Γ) and having been reflected on junction 2 (multiplication by S_{21}).

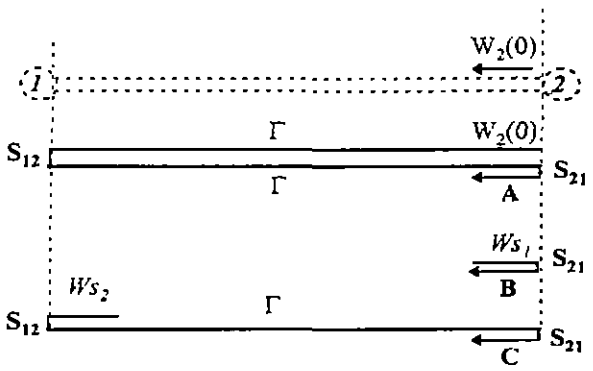

Fig. 5-2 : Expression of $W_2(0)$ as an addition of three wave terms, A+B+C

When $W_2(0)$ has been calculated, it becomes a source for the determination of the second unknown $W_1(0)$. So $W_1(0)$ can be easily calculated thanks to the first equation of (5-5) :

$$W_1(0) = S_{12}.\Gamma.W_2(0) + S_{12}.Ws_2 \qquad (5\text{-}7)$$

Figure 5-3 gives a graphical explanation of this equation. The disappearing of $W_2(0)$ unknown induces the disappearing of junction 2. As junction 2 does not exist anymore, it is not possible to find anymore possible paths propagating and scattering $W_1(0)$. However, it is still possible to say that $W_1(0)$ is equal to the summation of all the existing sources having propagated until arriving at the position of $W_1(0)$:

- source wave $A' = S_{12}.\Gamma.W_2(0)$
- source wave $B' = S_{12}.Ws_2$

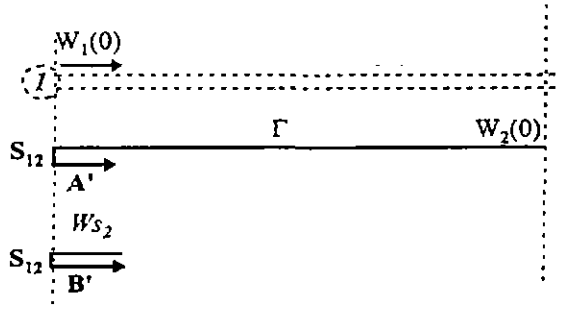

Fig. 5-3 : Expression of $W_1(0)$ after the determination of $W_2(0)$

For a more complex network, involving a greater number of tubes, the result would have been the same. This provides us the opportunity to define a rule we called the "***all-paths-and-sources***" rule. A wave W(z), taken at a z position, is equal to the sum of two types of terms :

1 - W(z) itself, having taken all the possible paths leading to the same position,
2 - all the source wave multiplied by the delay of all the paths leading to the "z" position.

This summation is exactly what an LU process does numerically. After the triangularization process, the last labeled unknown W_N equation obeys the rule previously expressed. Once calculated, this wave becomes a source with respect to the other unknowns. The W_{N-1} will then follow the same all-paths-and-sources rule, and so on.

5.2. Representing the BLT equation in a graph form

5.2.1. Representing the solution with graphs

Both the LU numerical process and topological networks can be represented with graphs. Again, let us consider the one tube topological network described on figure 5-1. Considering the two propagation equations given by (5-1) and the two scattering equations given by (5-3), one can easily express the system to solve as the flow graph described on figure 5-4.

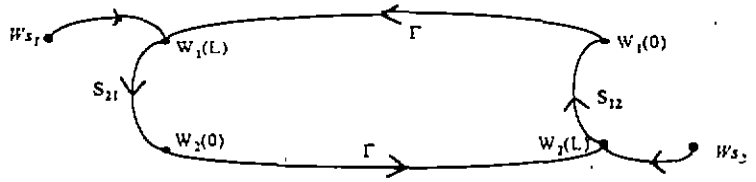

Fig. 5-4 : Flow-graph representation of the propagation and scattering equations on a tube

With this representation, we have an efficient tool to visualize the different paths involved in equations (5-6) and (5-7). Figure 5-5 shows the three successive paths (bold lines) leading to the calculation of $W_2(0)$ and figure 5-6 shows the two successive paths leading to the calculation of $W_1(0)$.

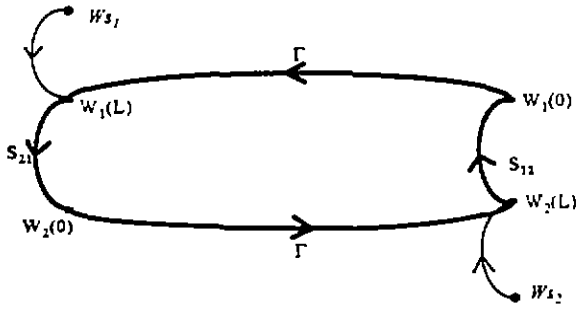

Calculation of wave A

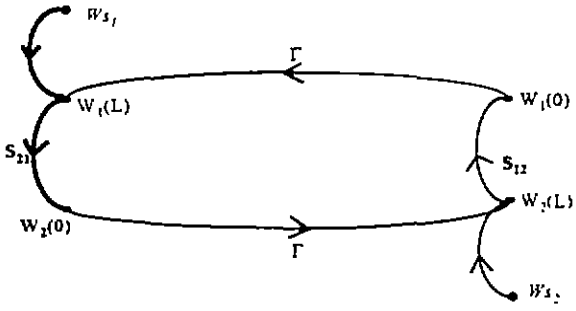

Calculation of source wave B

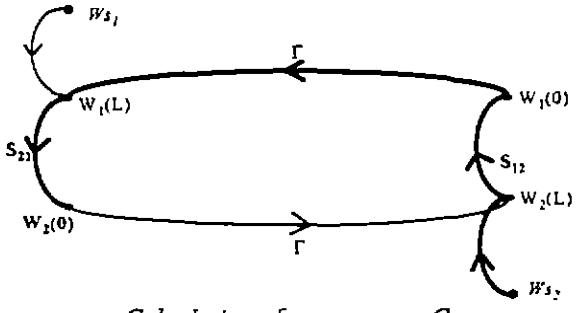

Calculation of source wave C

Fig. 5-5 : Different paths for the calculation of $W_2(0)$ with respect to figure 5-4 graph

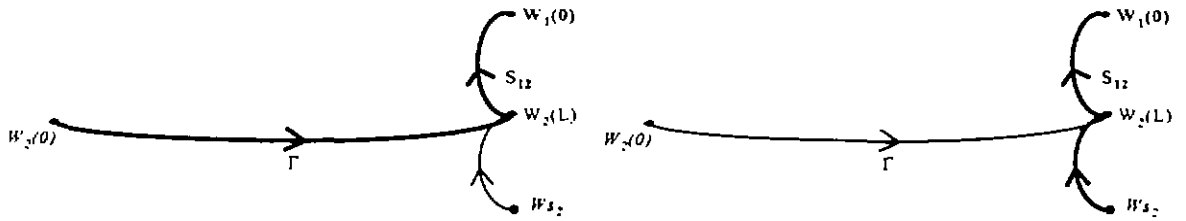

Calculation of source wave A' *Calculation of source wave B'*

Fig. 5-6 : Different paths for the calculation of $W_1(0)$ on figure 5-4 graph

5.2.2. Attempt to use classical flow-graph calculation rules

In the theory of linear systems, the use of flow graphs is widely spread. For instance the theory of flow graphs proposes elementary reduction rules which allow the simplification of complex graphs. More, general rules have been established by Mason [23] to calculate the transfer function, or so-called "gain", at any point of a graph, with respect to any source applied on this graph. Let us recall mason's rule. The rule supposes that a preliminary inventory of all the paths "k" relating the two variables involved in the gain and all the loops existing on the graph has been made. Then, the gain "G" between the two variables can be calculated by the following formula :

$$G = \frac{\sum_k G_k \cdot \Delta_k}{\Delta} \qquad (5\text{-}8)$$

wherein :

$$\Delta = 1 - \sum_m P_{m1} + \sum_m P_{m2} - \sum_m P_{m3} + \ldots + (-1)^{mr} \cdot \sum_m P_{mr}$$ is called the ***determinant***, (5-9)

P_{mr} = gain of the m^{th} possible combination of "r" non touching loops,

Δ_k = the value of Δ for that part of the graph non touching the k^{th} forward path, called ***cofactor*** of forward path k.

For our purpose, the problem of Mason's formula lays on the fact that it is valid only for scalar transfer functions, but not for matrix operators. Nevertheless, its application shows us how closely Mason's rule is related to the rule we previously called all-paths-and-sources rule. For example, for the determination of $W_2(0)$, assuming that each tube has only one component, the application of the Mason's rule on the one tube problem described on figure (5-4) would follow the different steps below:

1) Inventory of the loops : only one loop,
$P_{m1} = \Gamma.S_{12}.\Gamma.S_{21}$

2) Transfer function between $W_2(0)$ and Ws1 :

$G^1 = S_{21}$

3) Transfer function between $W_2(0)$ and Ws2 :

$G^2 = S_{21}.\Gamma.S_{12}$

So the application of (5-8) would give:

$$W_2(0) = (1 - \Gamma.S_{12}.\Gamma.S_{21})^{-1}.(G^1.Ws_1 + G^2.Ws_2) = (1 - \Gamma.S_{12}.\Gamma.S_{21})^{-1}.(S_{21}.Ws_1 + S_{12}.\Gamma.S_{21}Ws_2) \qquad (5\text{-}10)$$

which is entirely equivalent to (5-6) in the scalar case. In the general case of matrices, it is easy to figure out what order the different products appearing in (5-10) have to respect. However, even if the problem of the commutativity of the transfer function product was not a problem, the application of Mason's rule would become more complex for more than one tube network topology. Because network theory deals with two waves propagating on the same tube, many loops would quickly appear on the graph. To emphasize this remark, let us give the example of the BLT resolution on a two connected tube network (figure 5-7).

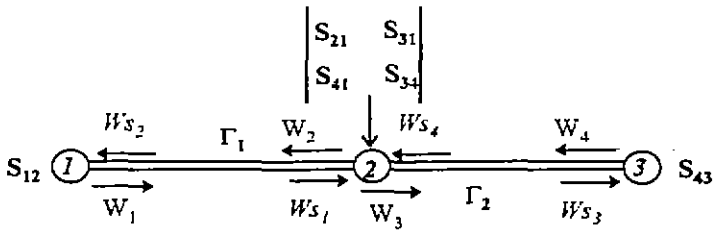

Fig. 5-7 : Two tube topological network

The BLT equation on figure 5-7 network can be simplified in the following form :

$$\begin{pmatrix} 1 & +a_{12} & 0 & 0 \\ +a_{21} & 1 & 0 & +a_{24} \\ +a_{31} & 0 & 1 & +a_{34} \\ 0 & 0 & +a_{43} & 1 \end{pmatrix} \cdot \begin{pmatrix} W_1 \\ W_2 \\ W_3 \\ W_4 \end{pmatrix} = \begin{pmatrix} S_1 \\ S_2 \\ S_3 \\ S_4 \end{pmatrix} \qquad (5\text{-}11)$$

where :

$$a_{12} = -S_{12}.\Gamma_1$$
$$a_{21} = -S_{21}.\Gamma_1$$
$$a_{31} = -S_{31}.\Gamma_1$$
$$a_{43} = -S_{43}.\Gamma_2$$
$$a_{24} = -S_{24}.\Gamma_2$$
$$a_{34} = -S_{34}.\Gamma_2$$
$$S_1 = S_{12}.Ws_2$$
$$S_2 = S_{21}.Ws_1 + S_{24}.Ws_4$$
$$S_3 = S_{31}.Ws_1 + S_{34}.Ws_4$$
$$S_4 = S_{13}.Ws_3$$

This equation is equivalent to the graph depicted on figure 5-8. This graph is nothing more than a reduction applied on propagation and scattering equations in order to eliminate waves $W_i(L)$, taken at the opposite ends of the tubes.

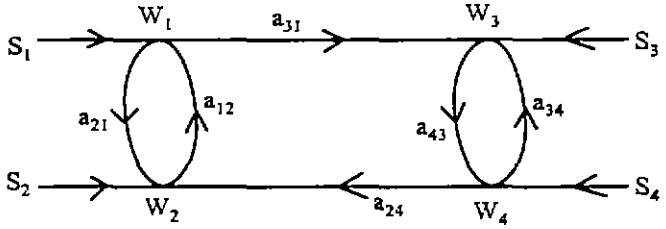

Fig. 5-8 : Graph representation of (5-11)

The LU process allows the determination of W_4. We obtain :

$$\left\{1-a_{43}.\left[a_{34}+a_{31}.a_{12}.\left(1-a_{21}.a_{12}\right)^{-1}\right].a_{24}.W_4 = \right.$$
$$S_4+a_{43}.\left[S_3+a_{31}.S_1-a_{31}.a_{12}.\left(1-a_{21}.a_{12}\right)^{-1}.\left(S_2+a_{21}.S_1\right)\right] \qquad (5\text{-}12)$$

The application of Mason's rule would have given :

1) Inventory of all the loops :

$T1 = a_{43}.a_{34}$

$T2 = a_{12}.a_{21}$

$T3 = a_{43}.a_{31}.a_{12}.a_{24}$

2) Inventory of non touching 2 loops

$T1.T2 = a_{43}.a_{34}.a_{12}.a_{21}$

3) Gain between W4 and S1 (multiplied by cofactor) :

$G^1 = a_{43}.a_{31}.(1 - a_{12}.a_{21})$

4) Gain between W4 and S2 (multiplied by cofactor) :

$G^2 = a_{43}.a_{31}.a_{12}$

5) Gain between W4 and S3 (multiplied by cofactor) :

$G^3 = a_{43}.(1 - a_{12}.a_{21})$

6) Gain between W4 and S4 (multiplied by cofactor) :

$G^4 = 1 - a_{12}a_{21}$

So, the application of (5-9) gives :

$$\left(1-a_{43}.a_{34}-a_{12}.a_{21}-a_{43}.a_{31}.a_{12}.a_{24}+a_{43}.a_{34}.a_{12}.a_{21}\right).W_4 = \qquad (5\text{-}13)$$
$$a_{43}.a_{31}.\left(1-a_{12}.a_{21}\right).S_1+a_{43}.a_{31}.a_{12}.S_2+a_{43}.\left(1-a_{12}.a_{21}\right).S_3+\left(1-a_{12}.a_{21}\right).S_4$$

Assuming that all the a_{ij} terms are scalar, the reader will check that (5-13) is fully equivalent to (5-12). Nevertheless, this simple example provides us two important lessons :

- because of the non commutatitivity between matrix operators, Mason's rule cannot be applied directly and one has to apply the all-paths-and-sources rule,
- whereas, its direct application becomes complex for networks made of more than one tube, the all-paths-and-sources rule is automatic and efficiently performed by the LU process.

5.2.3. Explanation of the fill-in with graph representation

Another interesting aspect of the flow graphs is that they give a tangible explanation of the fill-in creation process. Let us take the example described on figure 5-7 and let us generate a graph representation of the $\Pi_{u,v}$, characteristic matrix of the BLT equation (figure 5-9). This graph is closely related to the flow graph represented on figure 5-8. In this case, the difference is that, we only consider the interactions *between waves, without taking care of the value of the operators. Except for the self loops representing the* unit terms on the diagonal of the equation, this graph would be the same for the $W_{u,v}$ scattering characteristic matrix. On such a graph, it is easy to recognize that the two opposite arrows relating two

graph nodes represent the coupling between two junctions on the same tube. Figure 5-10 describes the different graphs obtained after the elimination of each wave, from W_1 to W_4. The fill-in appears in the elimination of W_1 graph, with the creation of a new branch from W_2 to W_3. The requirement to create this new branch is clear when we analyze figure 5-9. When eliminating W_1, we suppress a possible pass coming from W_2 to W_3 (through W_1). If we want the solution still to obey the all-paths-and-sources rule, we need to keep track of it in the reduced graph.

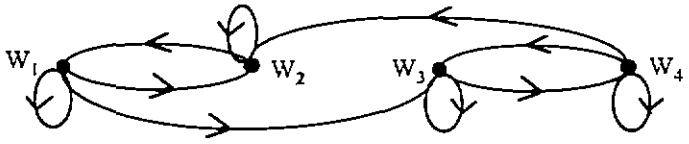

Fig. 5-9 : Representation of the $\Pi_{u,v}$ characteristic matrix of figure 5-7 network

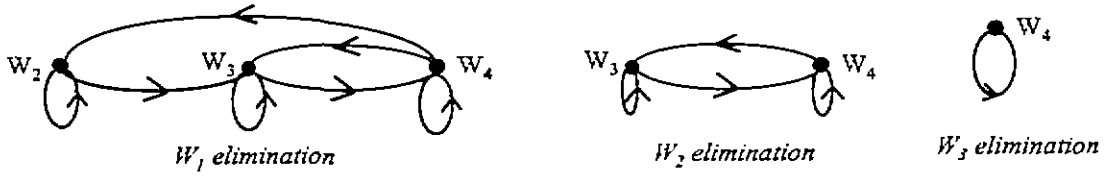

Fig. 5-10 : Graph representation of the $\Pi_{u,v}$ characteristic matrices of figure 5-9 graph

As a conclusion, we can say that the fill-in process is a way to keep track of all the possible paths existing on a network. From a graphical point of view, this phenomenon consists in the creation of new branches.

5.3. The BLT equation as a succession of subnetwork compacting steps

We saw that the general LU process is equivalent to eliminate the waves one after the other. In this section, we will suppose that the waves on each tube are labeled continuously as W_n and W_{n+1}. If now, the elimination of the waves is considered by groups of two waves belonging to the same tube, it is easy to figure out that the LU process will act as a succession of junction-to-junction compacting steps. Let us take the example of the two tube network described on figure 5-7. Previously, the BLT equation of this network has been presented in a condensed way (see (5-11)). For the purpose of this section, we will write the different steps of the triangularization process in its explicit form, involving the propagation and scattering matrix blocks.

Step 1 : original BLT equation

$$\begin{pmatrix} 1 & -S_{12}\Gamma_1 & 0 & 0 \\ -S_{21}\Gamma_1 & 1 & 0 & -S_{24}\Gamma_2 \\ -S_{31}\Gamma_1 & 0 & 1 & -S_{34}\Gamma_2 \\ 0 & 0 & -S_{43}\Gamma_2 & 1 \end{pmatrix} \cdot \begin{pmatrix} W_1(0) \\ W_2(0) \\ W_3(0) \\ W_4(0) \end{pmatrix} = \begin{pmatrix} S_{12}.Ws_2 \\ S_{21}.Ws_1 + S_{24}.Ws_4 \\ S_{31}.Ws_1 + S_{34}.Ws_4 \\ S_{43}.Ws_3 \end{pmatrix} \quad (5\text{-}14)$$

Step 2 : 1st column elimination

$$\begin{pmatrix} 1-S_{21}.\Gamma_1.S_{12}.\Gamma_1 & 0 & -S_{24}.\Gamma_2 \\ -S_{31}.\Gamma_1.S_{12}.\Gamma_1 & 1 & -S_{34}.\Gamma_2 \\ 0 & -S_{43}.\Gamma_2 & 1 \end{pmatrix} \cdot \begin{pmatrix} W_2(0) \\ W_3(0) \\ W_4(0) \end{pmatrix} = \begin{pmatrix} S_{21}.Ws_1 + S_{24}.Ws_4 + S_{21}.\Gamma_1.S_{12}.Ws_2 \\ S_{31}.Ws_1 + S_{34}.Ws_4 + S_{31}.\Gamma_1.S_{12}.Ws_2 \\ S_{43}.Ws_3 \end{pmatrix} \quad (5\text{-}15)$$

Step 3 : 2nd column elimination

$$\begin{pmatrix} 1 & -S_{34}.\Gamma_2 - S_{31}.\Gamma_1.S_{12}.\Gamma_1.(1-S_{21}.\Gamma_1.S_{12}.\Gamma_1)^{-1}.S_{24}.\Gamma_2 \\ -S_{43}.\Gamma_2 & 1 \end{pmatrix}.\begin{pmatrix} W_3(0) \\ W_4(0) \end{pmatrix} = \tag{5-16}$$

$$\begin{pmatrix} S_{31}.Ws_1 + S_{34}.Ws_4 + S_{31}.\Gamma_1.S_{12}.Ws_2 + \\ S_{31}.\Gamma_1.S_{12}.\Gamma_1.(1-S_{21}.\Gamma_1.S_{12})^{-1}.(S_{21}.Ws_1 + S_{24}.Ws_4 + S_{21}.\Gamma_1.S_{12}.Ws_2) \\ S_{43}.Ws_3 \end{pmatrix}$$

In the left part of (5-16) we recognize easily the BLT form of a single tube, in which the first tube of the original network, supporting W_1 and W_2 waves, has been compacted in an equivalent junction whose scattering parameters are (with respect to (3-1)):

$$S_{eq} = S_{34} + S_{31}.\Gamma_1.S_{12}.\Gamma_1.(1-S_{21}.\Gamma_1.S_{12}.\Gamma_1)^{-1}.S_{24} \tag{5-17}$$

Indeed, (5-17) obeys the general formulation of the subnetwork equivalent junction. In our case, the different matrix blocks involved in (3-1) are the following :

$$\Gamma_I = \begin{pmatrix} \Gamma_1 & 0 \\ 0 & \Gamma_1 \end{pmatrix} \tag{5-18}$$

$$S_{II,I} = S_{34} \tag{5-19}$$

$$S_{II,III} = \begin{pmatrix} S_{31} & 0 \end{pmatrix} \tag{5-20}$$

$$S_{III,I} = \begin{pmatrix} 0 \\ S_{24} \end{pmatrix} \tag{5-21}$$

$$S_{III,III} = \begin{pmatrix} 0 & S_{12} \\ S_{21} & 0 \end{pmatrix} \tag{5-22}$$

From the source point of view, the second component of the second member of (5-16) clearly shows that a non additional source wave has been created according to the $W_{II} = W_3$ direction, as respect with (3-4). The identification of the first component of the second member with the general definition of the equivalent source wave given in (3-5) is less straightforward and requires a specific mathematical treatment. In our case, the definitions of Ws_I and Ws_{III} are the following :

$$Ws_I = Ws_4 \tag{5-23}$$

and

$$Ws_{III} = \begin{pmatrix} Ws_1 \\ Ws_2 \end{pmatrix} \tag{5-24}$$

Using (5-18) to (5-23), the application of (3-5) gives in our example :

$$Wseq_{1\,(compactng)} = Seq.Ws_4 + S_{31}.Ws_1 + S_{31}.\Gamma_1.S_{12}.\Gamma_1.(1-S_{21}.\Gamma_1.S_{12}.\Gamma_1)^{-1}.S_{21}.Ws_1 + S_{31}.\Gamma_1.(1-S_{12}.\Gamma_1.S_{21}.\Gamma_1)^{-1}.S_{12}.Ws_2 \tag{5-25}$$

whereas, according to (5-16), the definition of the equivalent source wave calculated by the LU process gives :

$$Ws_{1\,(LU)} = Seq.Ws_4 + S_{31}.Ws_1 + S_{31}.\Gamma_1.S_{12}.\Gamma_1.\left(1-S_{21}.\Gamma_1.S_{12}.\Gamma_1\right)^{-1}.S_{21}.Ws_1 + \left(S_{31}.\Gamma_1.S_{12} + S_{31}.\Gamma_1.S_{12}.\Gamma_1.\left(1-S_{21}.\Gamma_1.S_{12}.\Gamma_1\right)^{-1}.S_{21}.\Gamma_1.S_{12}\right).Ws_2 \quad (5\text{-}26)$$

The only difference between (5-25) and (5-26) seems to be in the last term of the summation applying on Ws_2. If we make the following transformation in (5-26) :

$$X = S_{12}.\Gamma_1.S_{21}.\Gamma_1$$

we can demonstrate that both relations are fully equivalent :

$$\begin{aligned}
&S_{31}.\Gamma_1.S_{12}.\left(1+\Gamma_1.\left(1-S_{21}.\Gamma_1.S_{12}.\Gamma_1\right)^{-1}.S_{21}.\Gamma_1.S_{12}\right).Ws_2 = \\
&S_{31}.\Gamma_1.\left\{1+\left[\left(S_{21}.\Gamma_1\right)^{-1}.\left(1-S_{21}.\Gamma_1.S_{12}.\Gamma_1\right).\left(S_{12}.\Gamma_1\right)^{-1}\right]^{-1}\right\}.S_{12}.Ws_2 = \\
&S_{31}.\Gamma_1.\left[1+\left(\Gamma_1^{-1}.S_{21}^{-1}.\Gamma_1^{-1}.S_{12}^{-1}-1\right).^{-1}\right].S_{12}.Ws_2 = S_{31}.\Gamma_1.\left[1+\left(X^{-1}-1\right).^{-1}\right].S_{12}.Ws_2 = \\
&S_{31}.\Gamma_1.(1-X)^{-1}.S_{12}.Ws_2 = S_{31}.\Gamma_1.\left(1-S_{12}.\Gamma_1.S_{21}.\Gamma_1\right)^{-1}.S_{12}.Ws_2
\end{aligned} \quad (5\text{-}27)$$

This simple example demonstrates how a LU process can be seen as a the calculation of waves on a flow graph, and how, as well as a succession of compacting processes. The generalization to a more complex network becomes straightforward if one considers that in figure 5-7, junction 1 and source wave Ws_1 represent now an equivalent junction and equivalent source coming from the compacting of all the rest of the network.

As a conclusion, we can say that, what labeling waves on the same tube as W_n and W_{n+1}, the LU process is equivalent to eliminate the two wave set on each tube, one after the other. This is equivalent to say that the LU process, consists in a succession of a pairwise junction compacting steps.

6. Labeling waves on a network

6.1. Importance of wave labeling

As we saw in section 4.2, the LU process generates the creation of non-zero blocks. This phenomenon is known as fill-in. We mentioned that the location and the number of fill-in blocks strongly depend on the way unknowns are labeled on the network. Even if the number of initially non-zero blocks is not modified by the labeling, an improvement of the labeling could widely improve the memory requirement and the computation time required for the resolution of such a sparse linear problem [15] as the BLT equation. In this document, we will consider that the size of the blocks is big (typically more than10x10). Consequently, we can consider that the reduction of the number of fill-in blocks will always lead to a memory and calculation time improvement. This would not be always the case for small size blocks. Indeed, a full optimization would have to evaluate the time necessary for the inversion of each block. In this case, the research of the optimum quickly leads to prohibitive calculation times.

Most of the papers dealing with sparse matrices are numerical papers and have the objective to find the best labeling algorithm in order to perform ***parallel calculation***, involving several processors or computers.

For instance, the well-known technique named ***multifrontal*** deals with finding the maximum number of independent branches on a network, each branch being treated by a processor (([11], [24] and [25].

According to the way of thinking of EM topology which focuses on the systematic decomposition of problems in elementary problems in order to simplify its treatment, our purpose is different in the sense that we do not want necessarily to run parallel calculations. Consequently, to make the BLT equation more useful for many users, it would be suitable to be able to use it on single processor computers. In the past 10 years, many studies have demonstrated that EM topology provided all the tools for treating a large scale problem on limited computation means ([7], [9], [13]).

Before defining a labeling rule, we will first analyze the fill-in creation process on elementary network configurations : chain-subnetworks, branch-subnetworks and loop subnetworks.

6.2. Analysis of the fill-in process on elementary networks

6.2.1. Chain-subnetwork

In this section, we will call ***chain-subnetwork***, a subnetwork for which each junction is not connected to more than two tubes as described on figure 6-1. In this figure, waves have been labeled randomly. Figure 6-2 gives the $\Pi_{u,v}$ characteristic matrix of the BLT equation (see definition at section 2.). Fill-in blocks have been noted with an "*x*" character. For such a simple configuration, the fill-in obtained is relatively high (fill-in =10).

As we did in section 5.2.3, we will use graph representations to help to understand how the fill-in process happens (figure 6-3 and figure 6-4). The process deals with eliminating the waves in a progressive order, from W_1 to W_8. New branches are created to keep the memory of existing path between two nodes in the network. Those paths remain until all the branches related to those nodes are eliminated. For example, on figure 6-4, the graph representations show that the elimination of W_3 node creates itself three new branches.

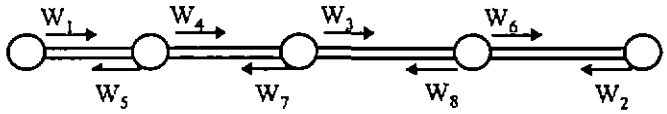

Fig. 6-1 : Example of chain-subnetwork with a random labeling

$$\Pi_{u,v} = \begin{pmatrix} 1 & 0 & 0 & 0 & 1 & 0 & 0 & 0 \\ 0 & 1 & 0 & 0 & 0 & 1 & 0 & 0 \\ 0 & 0 & 1 & 1 & 0 & 0 & 0 & 1 \\ 1 & 0 & 0 & 1 & x & 0 & 1 & 0 \\ 1 & 0 & 0 & 0 & 1 & 0 & 1 & 0 \\ 0 & 1 & 1 & x & x & 1 & x & x \\ 0 & 0 & 0 & 1 & x & 0 & 1 & 1 \\ 0 & 1 & 1 & x & x & x & x & 1 \end{pmatrix}$$

Fig. 6-2 : Characteristic matrix of the BLT equation for figure 6-1 subnetwork

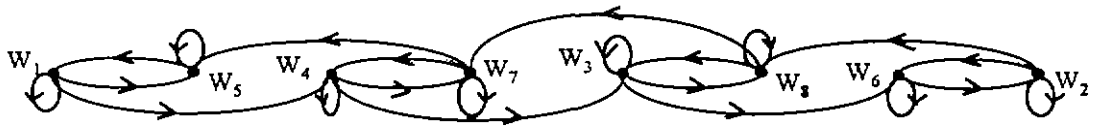

Fig. 6-3 : Graph representation of the BLT equation of figure 6-1

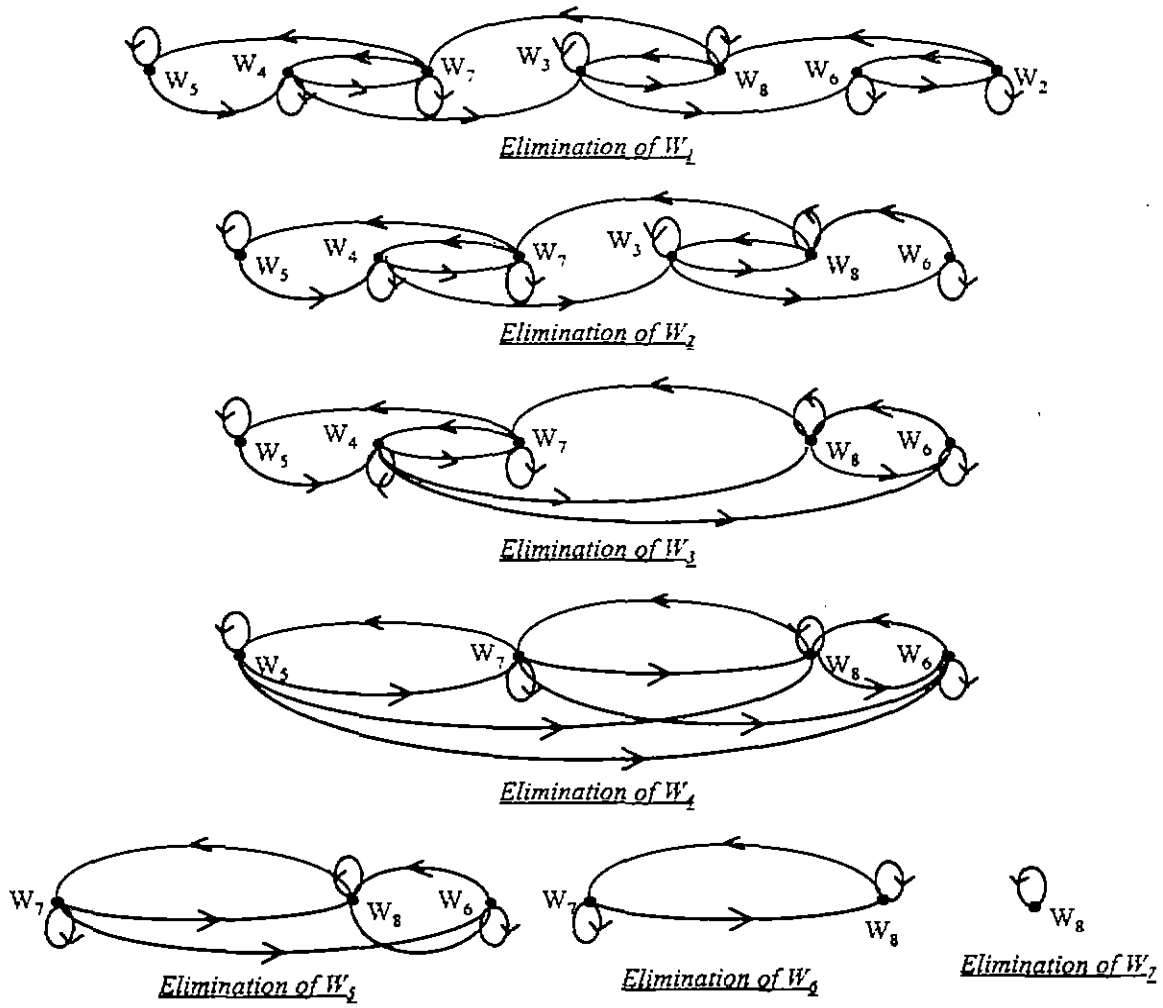

Fig. 6-4 : Different reduced graph for figure 6-1 BLT resolution

In the case of a chain-subnetwork, we see that, when a node W_i, connected to another node W_j, is eliminated on the graph, it would be better if the following elimination step was applied on W_j. Particularly, two branches connected to the same two nodes should be eliminated just one after the other. This remark is related to the elimination of a junction in a compacting process as described in section 5.3. Moreover, the newly created branches can be eliminated in the following elimination process, if the waves at the end of the graph are systematically eliminated.

Figure 6-6 shows the same subnetwork as figure 6-1, labeled in this sense. The characteristic matrix of the BLT equation is represented on figure 6-7. Compared figure 6-2, the fill-in is much smaller (3 instead of 10). The interest of this labeling is also that the fill-in appears in repetitive motives related to the connection of two tubes.

Figure 6-9 shows the different elimination steps on the related graph, described on figure 6-8. The branch created at one step always disappear in the next step. So they do not contribute to the creation of new branches anymore. The different steps presented on figure 6-9, are also equivalent to the elementary compacting of junctions on the network. By this way, in accordance to the fill-in calculated on figure 6-7, only three new branches are created in the elimination process.

From now, because of the importance of chain-subnetworks in network configurations, we will call ***tail-junctions***, the junctions connected to only one tube and ***chain-junctions***, the junctions connected to two tubes. These definitions come from the fact that the calculation of the compacting they offer is equivalent similar to the one provided with chain matrices ([21], [22]). The chain matrices can be used only on chain-junctions connecting two tubes only. On the contrary of scattering parameters they relate waves taken on the same tubes. As an example, according to figure 6-6 definition, we can define the chain matrix for the second junction from the left as :

$$\begin{bmatrix} W_3(0) \\ W_4(L) \end{bmatrix} = \begin{bmatrix} T_{31} & T_{32} \\ T_{41} & T_{42} \end{bmatrix} \cdot \begin{bmatrix} W_1(L) \\ W_2(0) \end{bmatrix} \tag{6-1}$$

Considering the scattering parameter matrix definition of the same junction, [S] ;

$$\begin{bmatrix} W_2(0) \\ W_3(0) \end{bmatrix} = \begin{bmatrix} S_{21} & S_{24} \\ S_{31} & S_{34} \end{bmatrix} \cdot \begin{bmatrix} W_1(L) \\ W_4(L) \end{bmatrix} \tag{6-2}$$

It is easy to demonstrate that we have the following relations :

$$[T] = \begin{bmatrix} S_{31} - S_{34} \cdot S_{24}^{-1} \cdot S_{21} & -S_{24}^{-1} \cdot S_{21} \\ S_{34} \cdot S_{24}^{-1} & S_{24}^{-1} \end{bmatrix} \tag{6-3}$$

and

$$[S] = \begin{bmatrix} -T_{42}^{-1} \cdot T_{41} & T_{42}^{-1} \\ T_{31} - T_{41} \cdot T_{42}^{-1} \cdot T_{32} & T_{32} \cdot T_{42}^{-1} \end{bmatrix} \tag{6-4}$$

The obvious interest in a chain matrix is that the chain matrix of two chain-junctions is nothing more than the product of the chain matrices of the two junctions. This way, the chain matrix of a whole chain-subnetwork can be easily calculated. Using (6-4), the scattering parameters of the equivalent network are then calculated giving the same result as (5-17). The simplicity of the chain matrix product is indeed closely related to the low fill-in rate generated by the chain-subnetworks. Nevertheless, strictly speaking of the BLT equation general formulation, originally expressed in terms of scattering matrices, the derivation of (3-1) and (3-5) are easier than the conversion of each junction scattering parameters into chain parameters, because they are automatically performed in the LU process.

Consequently, whatever calculation way is used to carry out the equivalent junction-to-junction compacting process, two main lessons have to be remembered from the chain-subnetwork analysis :

1 - waves have to be labeled successively on a same tube, to allow the elimination of junctions in a compacting process,

2 - waves have to be labeled successively from one tube to the other, to avoid new created branches participating to the fill-in process.

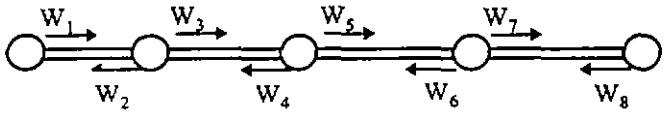

Fig. 6-6 : New labeling of figure 6-1 subnetwork

$$\Pi_{u,v} = \begin{pmatrix} 1 & 1 & 0 & 0 & 0 & 0 & 0 & 0 \\ 1 & 1 & 0 & 1 & 0 & 0 & 0 & 0 \\ 1 & x & 1 & 1 & 0 & 0 & 0 & 0 \\ 0 & 0 & 1 & 1 & 0 & 1 & 0 & 0 \\ 0 & 0 & 1 & x & 1 & 1 & 0 & 0 \\ 0 & 0 & 0 & 0 & 1 & 1 & 0 & 1 \\ 0 & 0 & 0 & 0 & 1 & x & 1 & 1 \\ 0 & 0 & 0 & 0 & 0 & 0 & 1 & 1 \end{pmatrix}$$

Fig. 6-7 : Characteristic matrix of the BLT equation for figure 6-6 subnetwork

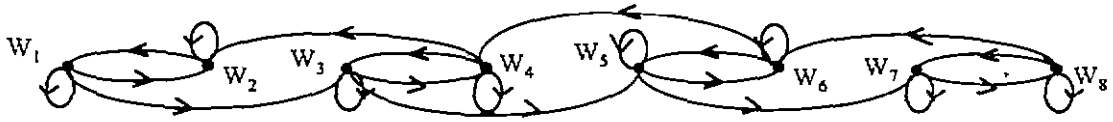

Fig. 6-8 : Graph representation of the BLT equation of figure 6-6

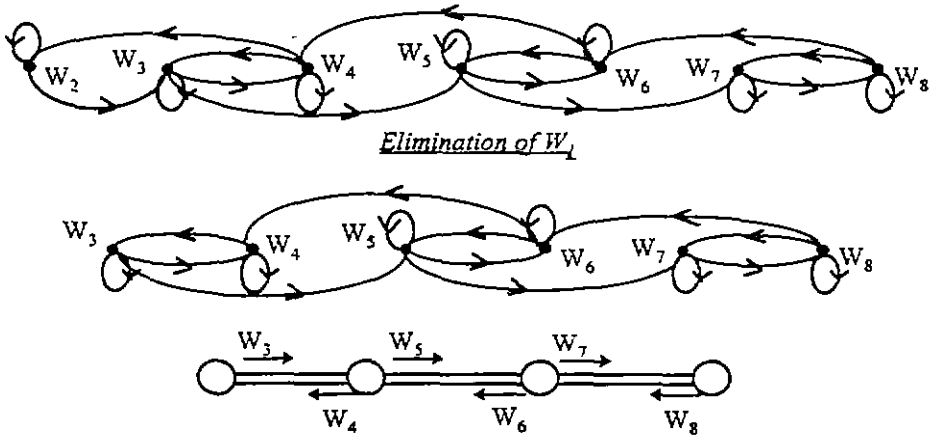

Fig. 6-9 : Different reduced graphs for figure 6-6 BLT resolution

6.2.2. Branch-subnetworks

It is interesting to analyze how the labeling rules previously defined for chain-subnetworks can be applied for branch-subnetwork, that is to say subnetworks involving several branches. With respect to the tail-junction and chain-junction definitions, we will call a ***branch-junction*** a junction connected to 3 or more tubes. Now, the successive labeling of two waves on the same tube is still possible, but, of course, the successive labeling on a junction is not applicable at the branch-junction level anymore.

Figure 6-10 gives an example of a labeling on a branch-subnetwork, involving one branch-junction, and its associated characteristic matrix. This matrix shows that waves W_3, W_4 and W_5 are eliminated before the waves located at the tail-junctions. This way, the existing paths between junction 3 and junction 5 have to be kept in memory during the elimination of W_3, W_4 and W_5 and thus lead to the creation of new branches. Consequently, the fill-in of figure 6-10 subnetwork is equal to 7 and can be optimized. One has only to notice that the previous drawback can be avoided if the waves at tail-junctions are eliminated as soon as possible. This remark is equivalent to the requirement of compacting all the tail-junctions existing on the original subnetwork or the newly created equivalent subnetwork. Because we saw at section 6.2.1 that waves had to be labeled successively on "***tail subnetworks***", the compacting will have to apply on each branch, from the tail junction. Figure 6-11 shows a new labeling of this subnetwork allowing such a wave elimination order and the associated BLT characteristic matrix. The fill-in is now much lower and is equal to 4. The interesting thing to notice is that no fill-in bloc participates to the creation of new fill-in blocs. This makes the matrix been constituted by two elementary sub-blocks :

- one for the branch configuration at the level of junction 2,
- one for the chain configuration at the level of junction 4.

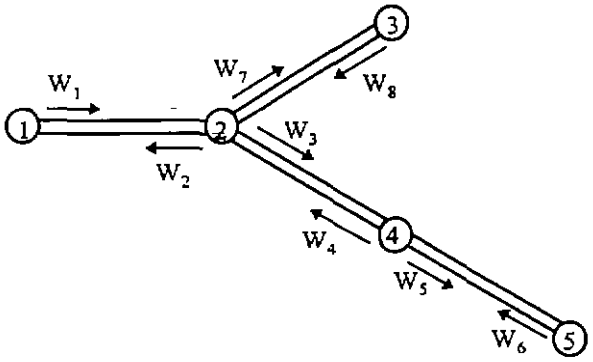

$$\Pi_{u,v} = \begin{pmatrix} 1 & 1 & 0 & 0 & 0 & 0 & 0 & 0 \\ 1 & 1 & 0 & 1 & 0 & 0 & 0 & 1 \\ 1 & x & 1 & 1 & 0 & 0 & 0 & 1 \\ 0 & 0 & 1 & 1 & 0 & 1 & 0 & x \\ 0 & 0 & 1 & x & 1 & 1 & 0 & x \\ 0 & 0 & 0 & 0 & 1 & 1 & 0 & x \\ 1 & x & 0 & 1 & 0 & x & 1 & 1 \\ 0 & 0 & 0 & 0 & 0 & 0 & 1 & 1 \end{pmatrix}$$

Fig. 6-10 : Example of a branch-subnetwork with its associated BLT characteristic matrix

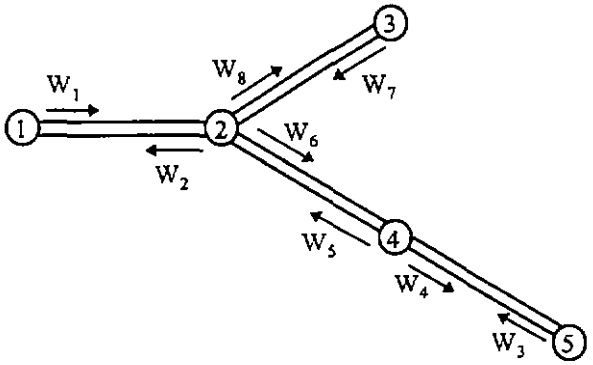

$$\Pi_{u,v} = \begin{pmatrix} 1 & 1 & 0 & 0 & 0 & 0 & 0 & 0 \\ 1 & 1 & 0 & 0 & 1 & 0 & 1 & 0 \\ 0 & 0 & 1 & 1 & 0 & 0 & 0 & 0 \\ 0 & 0 & 1 & 1 & 0 & 1 & 0 & 0 \\ 0 & 0 & 1 & x & 1 & 1 & 0 & 0 \\ 1 & x & 0 & 0 & 1 & 1 & 1 & 0 \\ 0 & 0 & 0 & 0 & 0 & 0 & 1 & 1 \\ 1 & x & 0 & 0 & 1 & x & 1 & 1 \end{pmatrix}$$

Fig. 6-11 : Optimized labeling on the branch-subnetwork of figure 6-10 and associated BLT characteristic matrix

As a conclusion for the analysis of branch-subnetworks, we can define two general rules to improve the labeling way of both chain and branch-subnetworks :

1 - waves have to be labeled successively on each tube. This rule had already been derived from the analysis of chain-subnetworks,

2 - waves on branches of branch-subnetworks have to be labeled successively from the tail junctions..

6.2.3. Loop subnetworks

We call ***loop subnetwork***, a subnetwork configuration for which two nodes connected by the same tube can also be connected by another path made by a series of different tubes. Figure 6-12 gives an example of a simple loop subnetwork configuration and its associated BLT characteristic matrix. The labeling of the waves follows the rules defined in the previous section. The problem with such a configuration is that, when compacting junctions one into the other, the first junction considered never becomes a terminal junction. From a graph point of view, this means that the wave elimination processes always have remember the path due to the loop. Consequently, the fill-in of such a configuration is necessarily high (equal to 10 in our example), and fill-in blocks contribute themselves to the creation of new fill-in blocks. Nevertheless, the two labeling rules defined in section 6.2.2 can be applied and still provide a significant fill-in improvement.

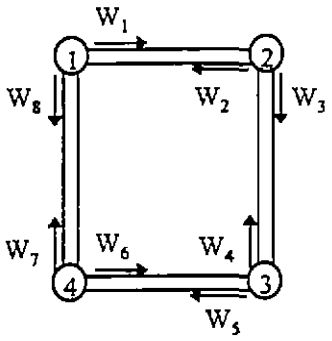

$$\Pi_{u,v} = \begin{pmatrix} 1 & 1 & 0 & 0 & 0 & 0 & 1 & 0 \\ 1 & 1 & 0 & 1 & 0 & 0 & x & 0 \\ 1 & x & 1 & 1 & 0 & 0 & x & 0 \\ 0 & 0 & 1 & 1 & 0 & 1 & x & 0 \\ 0 & 0 & 1 & x & 1 & 1 & x & 0 \\ 0 & 0 & 0 & 0 & 1 & 1 & x & 1 \\ 0 & 0 & 0 & 0 & 1 & x & 1 & 1 \\ 0 & 1 & 0 & x & 0 & x & 1 & 1 \end{pmatrix}$$

Fig. 6-12 : Example of a loop subnetwork and its associated BLT characteristic matrix

6.3. Definition of an improved labeling method

6.3.1. The chain-path-march rule

The analysis of labeling methods on elementary subnetworks has led us to define rules improving the fill-in. It has been shown that the labeling must allow a continuous elimination of the junctions by the automatic compacting of pair of junctions provided by the LU process. The labeling must be achieved in such a way that tail-junctions remain the less time as possible in the subnetworks on which the compacting is carried out. We also showed that these rules can still be applied to loop subnetworks, even if they do not provide the same improvement as for branch-subnetworks. The methods we propose give a significant reduction of the number of fill-in blocks, specially for chain and branch-subnetworks. In the case of loop subnetworks, it is hard to say that this method provides the optimum number of fill-in blocks. Nevertheless, it always provides a better fill-in than other classical methods.

To define the rule, we introduce the definition of a ***chain-path*** P(I,J) between two junctions I and J (I and J being a tail-junction or a branch-junction), as the succession of chain-junctions, allowing to connect the external junctions I and J of a chain-subnetwork. If a chain-path contains a tail-junction, we will call it a ***tail-path***. In the particular case of loop networks, any configuration of chain-path encountered on chain-networks and branch-subnetworks can be found, but chain-path can also relate two identical junctions. For example, we can write :

- P(2,5) = {2,4,5} ; P(1,2) ={1,2} ; P(3,2) = {3,2}, for figure 6-11,
- P(1,1) = {1,2,3,4,1} for figure 6-12.

Now, we can propose the following general recursive labeling method, we call the ***chain-path-march***, where "*march*" means here : *"label continuously the waves on the tubes connecting the chain-junctions of the path*". This method deals with creating "***reduced-subnetworks***". We call a reduced-subnetwork, a subnetwork containing all the tubes non already labeled in the process. Two kinds of reduced-subnetworks must be defined:

- ***branch-reduced-subnetworks*** : these subnetworks still contain tail-paths. The reduction of this subnetwork is performed by applying the ***tail-path-march***: this march is a chain-path-march applied on a tail-path. The reduction is made from the tail-junction of the tail-path.
- ***tail-irreducible-subnetworks*** : these subnetworks do not contain any more tail-paths. They subnetworks necessarily contain loops.

The recursive process we propose is decomposed in two steps :

- the creation of the irreducible subnetwork applying the tail march method,
- the reduction of the irreducible subnetwork applying the general chain march method.

It can be summarized by the following algorithm :

```
# Begin "Creation of an original tail-irreducible-subnetwork"
        #Do while tail-paths still exist
            # Begin "Reduced-subnetwork definition"
                # Make the inventory of all the remaining chain-paths
            End "Reduced-subnetwork definition" #
            # Begin "Reduction of tail-reduced-subnetwork"
                # March on all remaining tail-paths
            End "Reduction of tail-reduced-subnetwork" #
        End do #
End  "Creation of original tail-irreducible-subnetwork" #
                                                                    (6-1)
# Begin "Reduction of tail-irreducible-subnetworks"
        #Do while chain-paths still exist
            # Begin "Irreducible-reduced-subnetwork definition"
                # Make the inventory of all the remaining chain-paths
            End "Irreducible-reduced-subnetwork definition" #
            # Begin "Reduction of irreducible-reduced-subnetwork"
                # March on all remaining chain-paths
            End "Reduction of irreducible-reduced-subnetwork" #
        End do #
End "Reduction of tail  irreducible networks" #
```

Consequently, the labeling process is equivalent to a compacting process in which all the chain-subnetworks are systematically eliminated in one equivalent junction. The reduced-subnetworks are the equivalent networks obtained when introducing the equivalent junctions determined in the previous reduction step. The process is repeated until the reduced-subnetwork obtained is equal to a single junction.

6.3.2. Application on branch-networks

To demonstrate the application of the chain-path-march rule, let us first take the example of figure 2-1 network. This network does not involve any loop. Consequently, its reduction is limited to the first step in *section 6.3.1 algorithm. Here are the different chain-paths encountered on the original network. Figure 6-*13 presents the labeling obtained by the chain-path-march rule.

- P(1,3) = {1,2,3} ;
- P(9,3) = {9,3} ;
- P(5,3) = {5,4,3} ;
- P(7,6) = {7,6} ;
- P(8,6) = {8,6} ;

The reduced-subnetwork obtained contains only one chain-path ;

- P(2,1) = {2,1} ;

The final subnetwork is made of only one junction : junction 6.

The last junction of the chain-path always belongs to the newly created reduced-subnetwork. It must be noticed that the length of the chain is not important in the process, and for a given reduction step, chain-paths can be reduced in any order.

The resultant BLT characteristic matrix is presented on figure 6-14 and provides a significant improvement of the fill-in. As on figure 2-2, the fill-in blocks have been noted "x" and the originally non-modified diagonal blocks have been noted "$\underline{1}$". The fill in is now equal to 11 instead of 14, and the matrix is now 25 % filled. No fill-in block contributes to the creation of new fill-in blocks. Now we can say that the first labeling proposed on figure 2-2 was not so bad, especially because waves were labeled continuously on each tube.

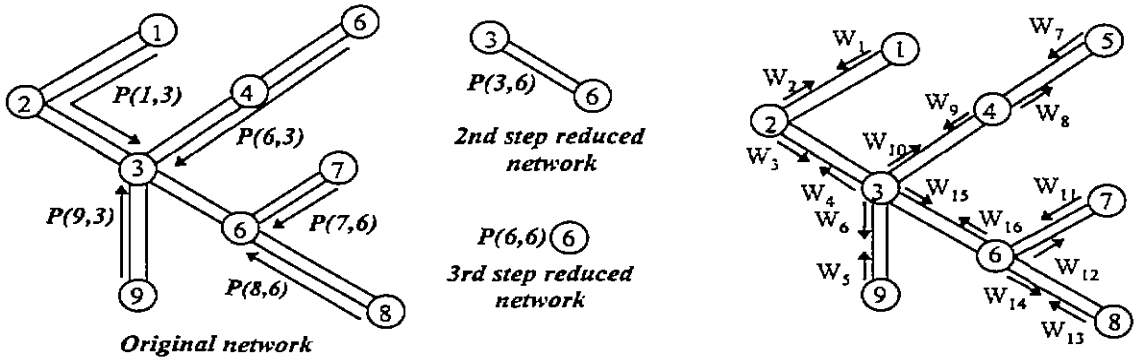

Fig. 6-13 : Application of the chain-path-march labeling method on figure 2-1 network

$$\Pi_{u,v=}\begin{pmatrix}
1 & 1 & 0 & 0 & 0 & 0 & 0 & 0 & 0 & 0 & 0 & 0 & 0 & 0 & 0 & 0\\
1 & \underline{1} & 0 & 1 & 0 & 0 & 0 & 0 & 0 & 0 & 0 & 0 & 0 & 0 & 0 & 0\\
1 & x & 1 & 1 & 0 & 0 & 0 & 0 & 0 & 0 & 0 & 0 & 0 & 0 & 0 & 0\\
0 & 0 & 1 & \underline{1} & 1 & 0 & 0 & 0 & 1 & 0 & 0 & 0 & 0 & 0 & 1 & 0\\
0 & 0 & 0 & 0 & 1 & 1 & 0 & 0 & 0 & 0 & 0 & 0 & 0 & 0 & 0 & 0\\
0 & 0 & 1 & x & 1 & \underline{1} & 0 & 0 & 1 & 0 & 0 & 0 & 0 & 0 & 1 & 0\\
0 & 0 & 0 & 0 & 0 & 0 & 1 & 1 & 0 & 0 & 0 & 0 & 0 & 0 & 0 & 0\\
0 & 0 & 0 & 0 & 0 & 0 & 1 & \underline{1} & 0 & 1 & 0 & 0 & 0 & 0 & 0 & 0\\
0 & 0 & 0 & 0 & 0 & 0 & 1 & x & 1 & 1 & 0 & 0 & 0 & 0 & 0 & 0\\
0 & 0 & 1 & x & 1 & x & 0 & 0 & 1 & \underline{1} & 0 & 0 & 0 & 0 & 1 & 0\\
0 & 0 & 0 & 0 & 0 & 0 & 0 & 0 & 0 & 0 & 1 & 1 & 0 & 0 & 0 & 0\\
0 & 0 & 0 & 0 & 0 & 0 & 0 & 0 & 0 & 0 & 1 & \underline{1} & 1 & 0 & 0 & 1\\
0 & 0 & 0 & 0 & 0 & 0 & 0 & 0 & 0 & 0 & 0 & 0 & 1 & 1 & 0 & 0\\
0 & 0 & 0 & 0 & 0 & 0 & 0 & 0 & 0 & 0 & 1 & x & 1 & \underline{1} & 0 & 1\\
0 & 0 & 0 & 0 & 0 & 0 & 0 & 0 & 0 & 0 & 1 & x & 1 & x & 1 & 1\\
0 & 0 & 1 & x & 1 & x & 0 & 0 & 1 & x & 0 & 0 & 0 & 0 & 1 & \underline{1}
\end{pmatrix}$$

Fig. 6-14 : BLT equation characteristic matrix for figure 6-13 network

6.3.3. Application on loop networks

The application of the recursive process explained in section 6.3.1 will always require at least the reduction of one irreducible network. Figure 6-15 gives an example of a network containing several loops. Two labeling ways of this network have been considered :

- the ***implicit labeling*** for which the waves are labeled in the order they are created in the network topology description. This means that the first created tube will support waves W_1 and W_2 ; the second created tube will support W_3 and W_4. And so on,
- the ***chain-path labeling*** applying the chain-path-march rule.

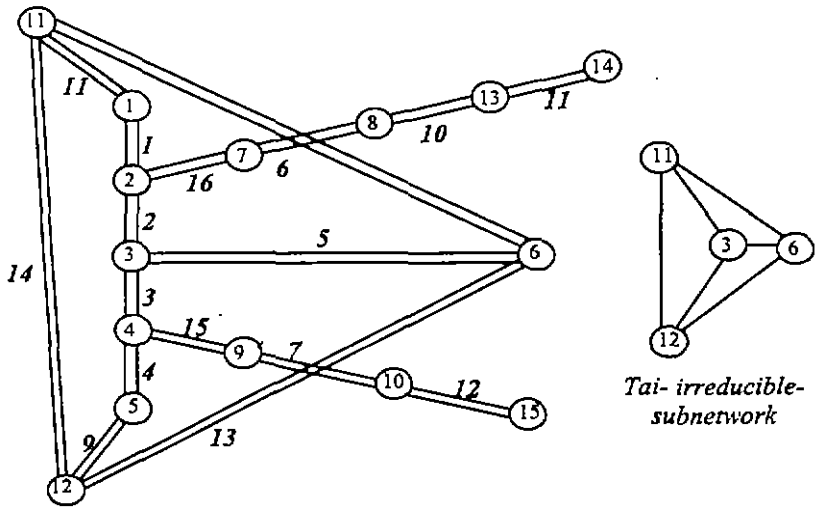

Fig. 6-15 : Example of a loop network requiring tail-path marching and general chain-path marching

The reduction process leads to the following network reduction :

1) Creation of the original tail irreducible network
- P(1,2) = {14,13,8,7,2}
- P(15,4) = {15,10,9,4}

2) Reduction of the irreducible network
- P(11,31) = {11,1,2,3}
- P(3,12) = {3,4,5,12}
- P(11,12) = {11,12}
- P(11,7) = {11,7}
- P(7,12) = {7,12}
- P(3,7) = {3,7}

One must notice that the irreducible network is the network defined by all the connections existing between junctions 3, 6, 11 and 12 (figure 6-15). Even if the fill in is bigger than in the case of branch-subnetwork, the chain-path method provides a better fill-in. The implicit method gives a fill-in equal to 163 whereas the chain-path method provides a fill-in equal to 82.

6.4. Application : calculation time improvements

6.4.1. General objectives

Taking into account the sparse property of the matrix is particularly useful for large size matrices. In this section we present different CRIPTE code calculations carried out on different networks. For each of them, we have written down the calculation times dealing with the different steps of the BLT equation. To manage with the different BLT calculation options presented in this paper, we introduce for each of them a specific encoding. Here are the different calculation steps we have checked :

- calculation of the ***tube*** matrices,
- calculation of the scattering parameters of ***junctions***,
- resolution of the ***BLT equation*** linear system :
    - option **D** : Direct method, without taking into account the sparse property of the matrix
    - option **S_Un** : taking into account the general Sparse properties of the matrix, treating Unit diagonal blocks as a common non-zero block
    - option **S_Uy** : taking into account the specific Sparse properties of the matrix (avoiding diagonal Unit blocks calculations),

For the calculations taking into account the sparse property of the BLT matrix, we have considered four different labeling methods. For each of these methods, the waves have been labeled continuously on each tube (as W_n and W_{n+1}). The labeling methods, all implemented in the CRIPTE code, are :

- option **Im** : the "***Implicit***" labeling method, already mentioned in section 6.3.3,
- option **Cm** :the "***Chain-path-march***" labeling method.
- option **Co** : the "***Coloring***" labeling method. This method is the one generally proposed to improve parallel calculation algorithm. It contributes to the generation of independent branches which can be treated separately [15]. Waves are labeled in such a way that connected tubes must not have continuous labeling. This way, different "color" families are created
- option **Mp** : the "***Minimum path***" labeling method. This particular method has for objective to minimize the distance of the off-diagonal blocks to the diagonal blocks. The recursive labeling process can be summarized as follows. One has to begin marching on the longest path on the network, the length of the path being defined as the number of the junctions involved in the path. When a branch-junction is encountered, all the paths have to be labeled, marching from the longest path. After this, the user marches again on the original longest paths. And so on.

Finally, with respect to the calculation type, the name of a BLT calculation type will apply the following rule : "*resolution type*"_"*labeling type*"_" *unit block calculation type*". For instance a configuration called "*S _Cm_Uy* " means a sparse resolution technique avoiding calculation on unit diagonal blocks with a chain march labeling method.

Three network configurations have been considered : chain-networks, branch-networks and a loop network. For the two first types of networks, we have tried to analyze the improvement obtained as a function of the number of tubes introduced in the network description.

6.4.2. Number of tube dependence : chain-networks and branch-networks

In this section we want to show the gain obtained on two generic network topologies by the different resolution techniques when the number of tubes increases. The different chain-network configurations are obtained by connecting one tube on a tail-junction (figure 6-16). Beginning with a simple three tube branch-network, the other configurations are obtained by adding two tubes connected on the same tail-junction (figure 6-17).

In all of these networks, we have taken the same tube model. Tail-junctions are 50 Ω scattering parameters (file "*ter50_20.s*"), chain-junctions and branch-junctions are ideal connections between the

wires on each tube (respectively "*con40.s*" and "*con60.s*"). The same transmission line, 1 meter long, with 20 conductors (file "*tube.t*") has been considered for all the tubes. Tubes and junctions have been chosen in such a way that their parameters are frequency dependent and must be calculated at each frequency. On each network, calculations have been achieved with the CRIPTE code at 5 frequencies between 300 kHz and 100 MHz : the calculation times displayed are an average of the time for those 5 frequencies. For each of them, the source considered has been the same : a serial 1 volt generator applied on wire 1 of tube 1. The version of the code used in the calculations does not involve any compiling optimization option.

For the chain and branch-configuration, the maximum number of tubes considered is equal to 19. Consequently, the maximum number of unknowns is equal to 760. There are 19 chain-network configurations (from 1 to 19 tubes) and 8 branch-network configurations (with 3, 5, 7, 9, 11, 13, 15, 17, 19 tubes). For the chain configuration, the *minimum path* labeling option was not worth considering because it gave the same labeling order as the *chain march* option. To have significant calculation times, computations have voluntary been carried out on a slow computer, a SUN SPARK ONE. The average time to carry out the 205 calculations is close to 15 days.

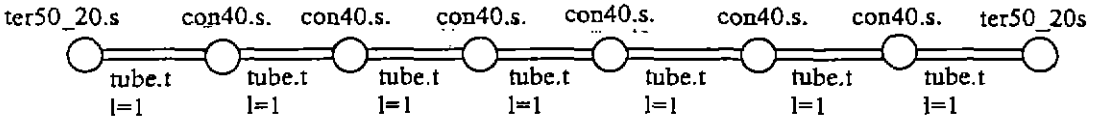

Fig. 6-16 : Generic chain network

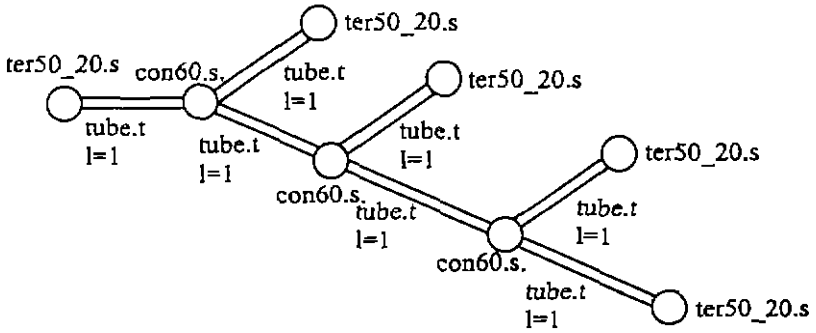

Fig. 6-17 : Generic branch-network

Figure 6-18 and figure 6-21 represent the calculation times with respect to the number of tubes for different critical steps of the BLT calculation. The gain brought by the sparse technique is obvious. One will notice the N^3 variation of the direct technique, which is a characteristic of LU technique (limit of the relation mentioned at section 4.1 when N is large), and which had been observed in many calculations performed with the previous versions of the CRIPTE code [9]. But the two sets of plots point out the fact that the improvement obtained with the sparse technique would soon require in the future the same kind of improvement for the calculation of scattering matrices of the junctions. The plots related to them clearly show their linear dependence with respect to the number of tubes. Nevertheless, let us recall that, in those calculations, we have forced the calculation of the scattering parameters and the characteristics of the tubes at each frequency and that no compiler option has been used to generate the code.

Figure 6-19 and figure 6-22 show the different calculation time obtained for different sparse techniques. Avoiding calculations on unit diagonal blocks always give better results than making the calculation on these blocks. The gain is particularly noticeable for chain matrices. For 19 tubes, the sparse matrix technique, using the chain-path-march labeling, is almost 50% faster than the implicit labeling technique for the chain-network and 25% faster for the branch-network. Figure 6-20 and figure 23 represent the fill-in obtained with respect to the number of tubes. The plots allow to setup a classification of the four labeling techniques for their efficiency to optimize the fill-in : 1^{rst}, chain-path-march labeling technique ; 2^{nd}, minimum path labeling technique ; 3^{rd}, colored path labeling technique ; 4^{th}, implicit labeling technique.

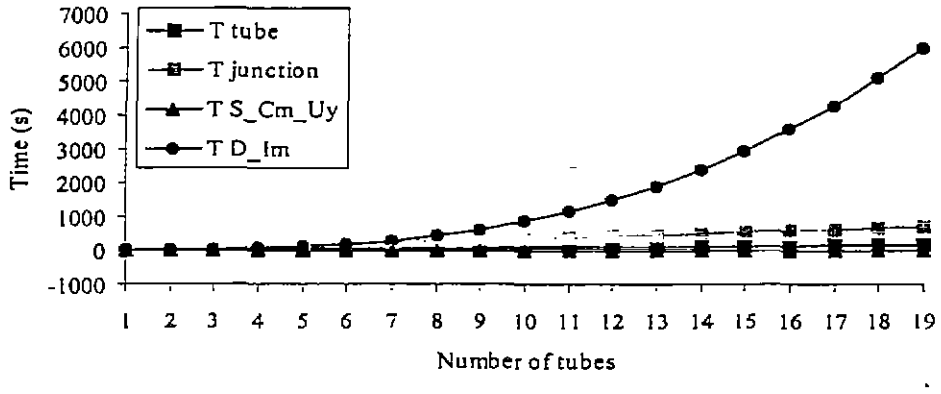

Fig. 6-18 : Chain-network configuration : computation times for direct and sparse LU resolution compared to tube and junction parameter calculation

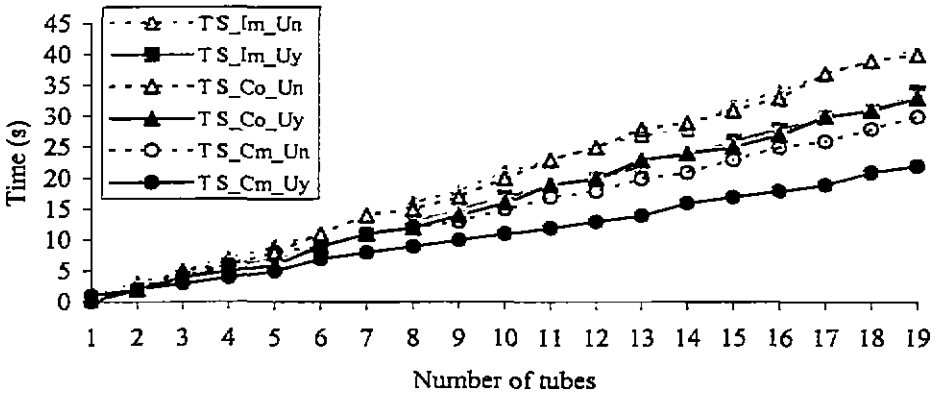

Fig. 6-19 : Chain-network configuration : calculation time for different sparse LU techniques

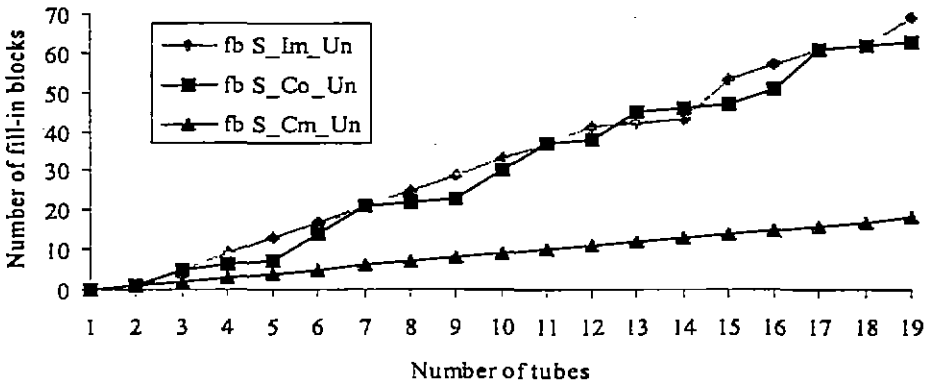

Fig. 6-20 : Chain-network configuration : fill-in per blocks for 3 labeling methods

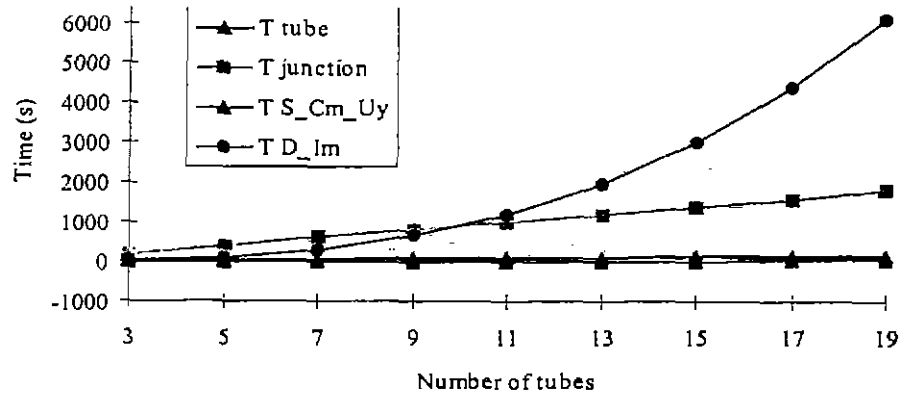

Fig. 6-21 : Branch-network configuration : computation times for direct and sparse LU resolution compared to tube and junction parameter calculation

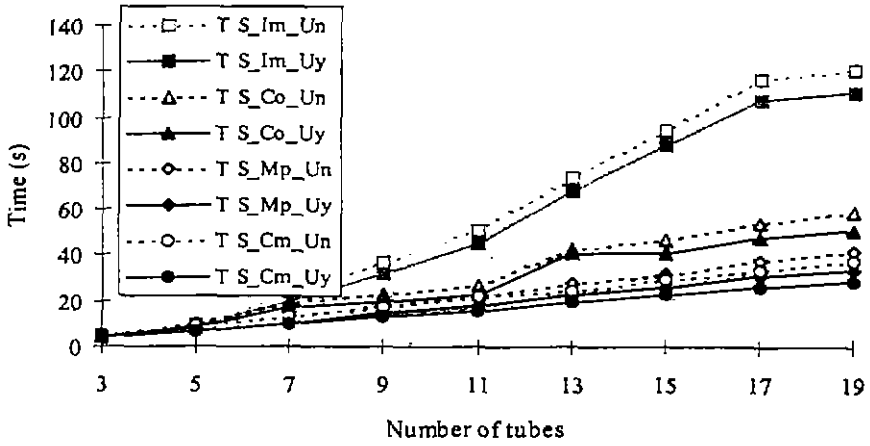

Fig. 6-22 : Branch-network configuration : calculation time for different sparse LU techniques

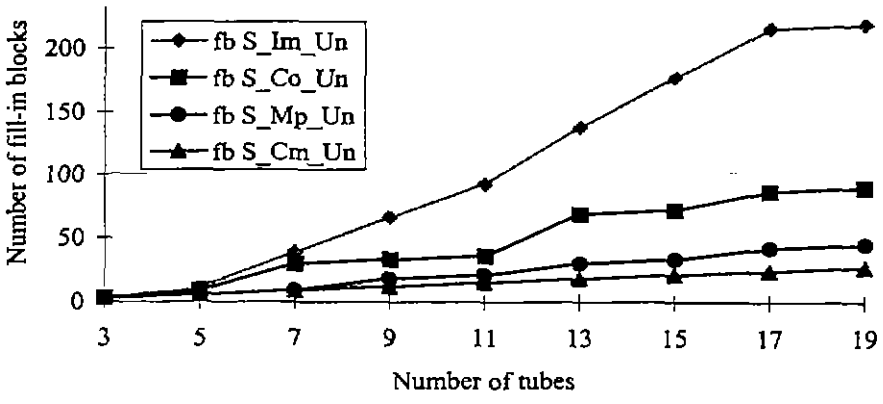

Fig. 6-23 : Branch-network configuration : fill-in per blocks for 4 labeling methods

6.4.3. Example of loop network

The loop example we have chosen in this section is the one depicted on figure 6-15. All the tubes have the same characteristics as the one used on section 6.4.2 networks (20 elementary wires). In the same way, the tail-junctions (14 and 15) have been applied the *ter50_20.s* file. The chain-junctions (1, 5, 7, 8 ,9,10, 13) have been applied the *con_20_20.s* file. And the branch-junctions (2, 3, 4, 6, 11, 12) have been applied the *con_20_20_20.s* file. The excitation is equal to a 1 volt serial generator applied at junction 14.

The fill-in obtained for the four previously mentioned labeling methods is reported on table 6-1. The calculations confirm the fact that the chain-path march method provides the smallest fill-in. The computation times for the BLT matrix inversion are reported on table 6-2 as the function of the type of calculation (see section 6.4.1 for the encoding of the calculation type). Avoiding calculation on unit blocks still provides an improvement. Again, as for chain and branch-networks, the important fact is that the junction scattering parameter calculation limits the total computation time in the sparse matrix technique. Nevertheless, a test has been performed using a version of the CRIPTE code compiled with an optimization option of the compiler. The time to calculate the junction was the equal to 5 min. 14 s. and the BLT equation resolution time on the S_Im_Uy configuration was lowered to 13 s.

Labeling	Implicit	Coloring	Minimum path	Chain-path-march
Fill-in	163	123	91	82

Table 6-1 :Fill-in obtained for figure 6-15 loop network

Labeling	Implicit	Coloring	Minimum path	Chain-path-march
Tubes	2 min. 25 s.	2 min. 25 s.	2 min. 25 s.	2 min. 25 s.
Junctions	24 min. 25 s.	24 min. 25 s.	24 min. 25 s.	24 min. 25 s.
D_xx	1 h. 13 min. 01 s.	x	x	x
S_xx_Un	1 min. 34 s.	1 min. 19 s.	1 min. 00 s.	58 s.
S_xx_Uy	1 min. 27 s.	1 min. 13 s.	53 s.	52 s.

Table 6-2 : Calculation times obtained for figure 6-15 loop network

7. Conclusion

In this work, more than the presentation of a numerical resolution of a linear system, we have tried to emphasize different ways to understand the significance of an LU technique applied to the BLT equation. We have also shown how this technique could be generalized to the powerful compacting of subnetworks. But we also wanted to demonstrate that it was.

First, with the same routine used to solve a BLT equation, we showed that scattering parameters and equivalent sources could be derived on any subnetwork. The natural LU method we used to solve the BLT equation, hides very interesting physical properties. Using flow-graph theory, we have shown that the LU process is equivalent to express the wave on a network as the sum of all the possible paths scattering this wave on the network and possible sources arriving to its location. The similarity with famous calculation rules, such as Mason's rules, well known in the domains of electric circuits and automatism has been mentioned. It could have been a great help for the resolution of the equation but it is valid only for scalar variables. So, this rule does not fit with the matrix block formulation of the BLT equation.

Second, the bi-directed coupling existing on tubes suggests a way to label waves continuously on a same tube. This way, the analysis of the analytical solution and the analysis of the related flow-graph demonstrated that the LU process automatically provides a real junction-to-junction subnetwork compacting.

We have also emphasized the fact that the sparse structure of this equation allows different computation improvements. Taking it into account gives significant reduction of memory requirement and calculation time. Moreover, due to its specific formulation, particular calculations dealing with unit diagonal blocks can be avoided. But, the most significant improvement is certainly that the junction-to-junction compacting operation hidden in the LU process suggests an intuitive way to label the waves on a network to reduce the number of fill-in blocks created.

In the past few years, electromagnetic topology had proved it was an efficient method to treat EM coupling on large scale problems. Thanks to the subnetwork compacting capability, it was always possible to decompose a big system in small systems. However, the desire to keep running the BLT equation on small computers, required numerous subnetwork calculations, increasing the number of network manipulations, the number of calculations, and the number of intermediate data to store. Now, the new considerations on the sparse structure of the BLT equation allow one to avoid all these drawbacks and, in the future, will make the user more inclined to apply the method on industrial type problems.

Meanwhile, these improvements open new theoretical application fields to electromagnetic topology:

- the generation of statistical data-bases because of the capability to run numerous calculations on different configurations of the same network,
- the resolution of inverse problems based on multiple source state excitations on the networks,
- the implementation of the non-uniform BLT (NBLT) equation, which takes into account non-uniform bundles, because the theory lays on the calculation of chain matrices,
- the generalization of the applications of network calculations on 3D structures with their large block requirements.

Tomorrow, because the computation requirements will no longer be a problem, EM topology and the use of network theory will go on spreading in laboratories. It will also be able to extend its applications to low frequency problems (the site protection against lightning for example) and high frequency problems (the treatment of an aircraft up to several GHz for example).

References

[1] C. E. Baum : The Theory of the Electromagnetic Interference Control. Interaction Notes. Note 478, December 1989 and, Modern Radio Science 1990, pp. 87-101, Oxford University Press.

[2] C. E. Baum, T. K. Liù, F. M. Tesche : On the Analysis of General Multiconductor Transmission-Line Networks, Interaction Notes, Note 350, November 1978; also in C.E. Baum, Electromagnetic Topology for the Analysis and Design of Complex Electromagnetic Systems, pp. 467-547 in JE. Thomson and H. Leussen (eds.), Fast Electrical and Optical measurements, Vol. 1, Martinus Nijoff, Dordrecht, 1986.

[3] J. P. Parmantier, G. Labaune, J. C. Alliot, P. Degauque : Electromagnetic Topology on Complex Systems: Topological Approach, Interaction Notes, Note 488. May 1992 and in La Recherche Aérospatiale, 1990, n°5, pp. 57-70.

[4] J .P. Parmantier : Approche Topologique pour l'étude des couplages électromagnétiques, Ph.D. report of Lille Flandres Artois University, December 1991. (in French - English translation available at ESA)

[5] J. P. Parmantier, P. Degauque : Topology Based Modeling of Very Large Systems, Modern radio Science 1996. Edited by J. Hamelin. Oxford University Press. pp. 151-177.

[6] J. P. Parmantier : Recent Developments in Electromagnetic Topology. 3rd ESA Workshop on EMC, EM Modelling for System Analysis. Pisa (Italy). 26-28 September 1993. pp. 3-10.

[7] J. P. Parmantier, V. Gobin, F. Issac, I. Junqua, Y. Daudy, J.M. Lagarde : An Application of the Electromagnetic Topology Theory on the Test-bed Aircraft, EMPTAC, Interaction Notes, Note 506, November 1993.

[8] J. P. Parmantier, V. Gobin, F. Issac, I. Junqua, Y. Daudy, J.M. Lagarde : Analysis of EM. Coupling on Large Structures Using E.M. Topological Concepts : Application to the EMPTAC Aircraft. Proceedings of ICEAA95 symposium. Politecnico di Torino (Italy). 12-15 September 1995, pp. 81-84.

[9] J. P. Parmantier, V. Gobin, F. Issac, I. Junqua, Y. Daudy, J.M. Lagarde : ETE III : Application of Electromagnetic Topology on EMPTAC, Interaction Notes, Note 527, May 1997.

[10] CRIPTE code users guide, ESI/ONERA, 1997

[11] X. Ferrières, B. L. Michielsen : Résolution efficace des équations de lignes de transmission pour réseaux complexes, Proceedings of the French EMC meeting. Toulouse, 2 - 4 ,March 1994 (in French).

[12] C. E. Baum : Generalization of the BLT equation, Interaction Notes, Note 511, 11 April 1995.

[13] L. Paletta, P. Dumas, J. P. Parmantier : Utilisation du champ électromagnétique tangentiel comme terme source dans les problèmes de Topologie Electromagnétique, Proceedings of the French CEM meeting, Lille, 3-5 September 1996, pp. 241-248. (in French).

[14] J. N. Franklin : Matrix Theory, Pentice-Hall Series in Applied Mathematics, 1968

[15] I. S. Duff, A.M. Erisman : Direct Methods for Sparse Matrices, Clarendon Press. Oxford, 1986.

[16] E. A. Guillemin : Theory of Linear Physical Systems, John Wiley & Sons Inc. 1963.

[17] C. E. Baum : The Role of scattering Theory in Electromagnetic Interference Problems, in Electromagnetic Scattering, Edited by P. L. E. Uslenghi, Academic Press. pp. 471 to 502, 1978

[18] J. P. Parmantier, G. Labaune, J. C. Alliot, P. Degauque : Electromagnetic Topology: Junction Characterization Methods, Interaction Notes, Note 489. May 1992 and in La Recherche Aérospatiale, 1990, n°5, pp. 71-82.

[19] J. P. Parmantier, R. Conduché : Couplages de méthodes linéaires et non linéaires, Proceedings of the 8th EMC French Symposium, Lille (France), September 1996, pp. 249-254 (In French).

[20] J. P. Parmantier, S. Bertuol, X. Ferrières : Développements de modules de calcul dans le logiciel CRIPTE: - câble blindé, - onde plane, - RSIL, ONERA's report, RTS n°16/6727 PY, January 1997. (in French).

[21] S. Ramo, J. R. Whinnery, T. Van Duzer : Fields and Waves in Communication Electronics, John Wiley & Sons, 1965, 1984, 1994.

[22] J. P. Parmantier : Méthodes pour le traitement du couplage électromagnétique sur le câblage d'un système de grande dimension, ONERA's report, RTS 12/6727 PY, February 1996. (In French).

[23] S. J. Mason : Feedback Theory - Further properties of Signal Flow Graphs, Proceedings IRE, 1956, 44(7), 920-926 and in Circuit Theory, edited by M. E. Van Valkenburg. Dowden, Hutchinson & Ross, Inc. 1974, pp. 295 to 301.

[24 I.S. Duff : Sparse Matrices and their Uses, Academic Press, New York and London 1984

[25] S. T. Hadfield : On the LU Factorization of Sequences of Identically Structured Sparse Matrices within a Distributed Memory Environment, Ph.D. report of the University of Florida. 1994.